Role of miR-31 in Metastatic Phenotypes of Cutaneous Squamous Cell Carcinoma

Undergraduate Research Thesis

Presented in Partial Fulfillment of the Requirements for graduation “with Honors Research Distinction in Biology” in the undergraduate colleges of The Ohio State University

by
Gwenyth Amborski

The Ohio State University
May 2020

Project Advisor: Dr. Amanda E. Toland, Ph.D., Department of Cancer Biology and Genetics

ABSTRACT

Metastatic cutaneous squamous cell carcinoma (cSCC) is rare but deadly, leading to an estimated 3,932 to 8,791 deaths in the United States annually. Changes in microRNA (miRNA) expression have been found in every cancer and are associated with tumor development and metastasis. A Toland lab study investigated miRNA expression in cSCCs isolated from sites associated with metastasis (aggressive sites), cSCCs at sites with lower risk for metastasis (non-aggressive sites), and non-tumor skin tissue. miR-21, let-7g, miR-93, miR-22, and miR-31 showed different expression between aggressive and non-aggressive sites. A literature search suggested that these miRNAs could play a role in the aggressiveness of tumors. miR-31 was one of the miRNAs that was upregulated in anatomical sites associated with cSCC metastasis. The upregulation of miR-31 at sites associated with metastasis led to the further investigation of its role in tumor and metastatic phenotypes in this study. Through literature and miRNA target database searches, we identified genes regulated or predicted to be regulated by miR-31. Many of these genes are part of the p38/MAPK pathway which has been reported to control some common metastatic phenotypes. Based on these studies, I hypothesized that an increase in miR-31 expression would lead to an increase in metastatic phenotypes via the p38/MAPK pathway. The goal of this study was to evaluate metastatic phenotypes and determine whether miR-31 regulates p38/MAPK genes in keratinocyte or cSCC cells and if these genes were involved in any observed phenotypes. miR-31 expression was measured in HaCat (an immortalized keratinocyte cell line) and SRB-12 (a cSCC cell line) cells using quantitative real-time PCR (qPCR). Using transfection of miR-31 precursors or antagonists, miR-31 was overexpressed or inhibited in these cells. Western blot analysis was used to measure any post-translation

effects on candidate miR-31 targets. Migration and proliferation assays were performed to measure metastatic characteristics. Endogenous miR-31 was upregulated in SRB-12 cells 2.6-fold (p-value=0.06) compared to HaCaT cells. qPCR analysis showed no significant expression differences between cells with or without miR-31 expression and the predicted miR-31 target genes: *MAPKAPK2, DUSP7, STAT3, MAP3K1, MAPK14, MAP2K4, MEF2A, and CREB1*. qPCR results showed a link between increased miR-31 levels and decreased *LIMK2* expression in the HaCaT cell line. MTT assays showed no conclusive differences in proliferation between HaCaT cells with or without miR-31 expression. However, migration assays showed that HaCaT and SRB-12 cells transfected with miR-31 experienced gap closure before cells transfected with anti-miR-31. In summary, increased miR-31 expression leads to an increase in the migration of HaCaT and SRB-12 cells, suggesting that miR-31 may contribute to this metastasis-related phenotype. Of the target genes, we only observed a weak correlation between *LIMK2* expression and miR-31. Future studies will determine if MAPK pathway gene, *LIMK2*, or other untested miR-31 target genes are important for metastatic phenotypes.

TABLE OF CONTENTS

LIST OF FIGURES

LIST OF TABLES

CHAPTER 1: INTRODUCTION

1.1 Cutaneous Squamous Cell Carcinoma

Cutaneous squamous cell carcinoma (cSCC) is a form of skin cancer arising from keratinocytes. In Caucasians, it is the second most common form of skin cancer. [1] Incidence of cSCC has been rising in previous years; cSCC incidence has increased by 263% from the 1976-84 timeframe to the 2000-10 timeframe. [2] A frequent location of this cancer is on the head and neck; this could be due to increased exposure to UV radiation. [1] For example, in one study with 772 primary cSCC tumor samples, 96.5% of the tumors were located in a sun-exposed region on the head or neck. [3] Other factors that lead to a higher rate of cSCC are genetic predisposition, immunosuppression, and chemical carcinogen exposure. [1]

Cutaneous squamous cell carcinoma is derived from actinic keratoses. [3-5] Actinic keratoses are cancer precursors found on sun damaged skin. They present as keratinocytes with abnormal nuclei and disorganized growth that leads to a thickened stratum corneum, the top layer of the epidermis. Mutations in genes that regulate the cell cycle- *p53, p16, CDK4, STAT3*- are thought to cause the precursor actinic keratoses to develop into primary cSCC and may also influence the development of metastatic cSCC. [5]

Although the morbidity of cSCC is increasing, the mortality is generally low. In 2020, only 0.002-0.004% of the U.S. white population died from cSCC. [6] However, the development of metastatic cSCC increases disease-associated mortality. Metastatic cSCC is rare but deadly, leading to an estimated 3,932 to 8,791 deaths in the United States each year. About 70% of cSCCs that metastasize to distal sites

lead to death. [5] Typical locations of cSCCs that become metastatic are the lip, ear, nose, temple and the front of the scalp. [1]

1.2 miR-31

microRNAs (miRNA) are non-coding RNAs that regulate gene expression. They are about 22 nucleotides long and typically interact with the 3' untranslated region (UTR) of target mRNAs. miRNAs are known to degrade mRNAs, repress translation of proteins, and thus suppress gene expression. Although, under specific conditions they can also activate gene expression. [7,8]

The main pathway of miRNA biogenesis is the canonical pathway (Figure 1). Primary miRNAs (pri-miRNA) are processed into precursor miRNAs (pre-miRNA), and finally transformed into mature miRNAs. Transcription of host genes lead to pri-miRNAs. These pri-miRNAs are then cleaved by the enzyme Drosha at the hairpin structure to make pre-miRNAs. The pre-miRNAs move to the cytoplasm where the endonuclease Dicer removes the terminal loop to generate the mature miRNA. The mature miRNA is then loaded into the miRNA-induced silencing complex (RISC). This complex targets complementary sequences mRNA for degradation. Fully complementary sequences result in degradation of the mRNA. When some mismatches are present, which is the majority of interactions in animal cells, this will lead to the repression of translation and eventually degradation by other complexes. [7,8]

Changes in microRNA expression have been found in almost every cancer. [10] Many studies have been done to evaluate miRNAs in cancer diagnosis and prognosis as well as potential therapies or therapeutic targets. The majority of

miRNAs are found in the cell but some are located in extracellular fluids, like plasma, serum, saliva, cerebrospinal fluid, and urine. These circulating miRNAs can be used as biomarkers to detect diseases. [7]

miR-31 can act like a tumor suppressor or oncogene depending on the cell type. In triple negative breast cancer, miR-31 is downregulated and can inhibit metastasis. [11] Head and neck SCC and colorectal cancer both show upregulation of miR-31 compared to normal tissues. [12,13] In cSCC, miR-31 has been previously described to act as an oncomiR which is a miRNA associated with cancer, and it is upregulated in tumors. [12,14,15] miR-31 was previously shown to target genes that influence cell cycle, metabolism, apoptosis, and DNA repair including *FIH* and *RhoBTB1*. [12,14] Recent studies have presented miR-31 as a regulator of metastasis and metastatic phenotypes like migration, invasion, and colony formation. The ability of cells to multiply, form colonies, move out of the primary tumor site, and invade other tissues is a crucial part of metastasis. [15] While there has been a strong link between miR-31 and metastasis in many cancer types, including cSCC, there has been little research into the gene targets of miR-31 that lead to these phenotypes.

1.3 p38/MAPK pathway

The mitogen-activated protein kinase (MAPK) pathway has three familial subsets. These include the extracellular signal-regulated kinase (ERK), Jun kinase (JNK/SAPK) and p38 MAPK. [16] This is a complex signaling pathway with linkage to many genes as well as other pathways. Dysregulation of the MAPK pathway is not uncommon in cancers. The MAPK pathway in its simplest form is a protein

kinases cascade. An outside signal activates mitogen-activated protein kinase kinase kinases (MAPKKK) to phosphorylate and activate MAP kinase kinases (MAPKK) which then phosphorylate and activate MAP kinase (MAPK) that can then produce a biological response. [16] The different families of the MAPK pathway are defined based on the stimulus that triggers them into the cascade. The ERK pathway is activated by growth factors. The JNK pathway is activated by environmental stressors, inflammatory cytokines, and growth factors. The p38 pathway is primarily stimulated by environmental stressors, like UV radiation, and inflammatory cytokines. [17] (Figure 2)

The p38 pathway plays a role in many cellular responses that are important in cancer progression. These include apoptosis, differentiation, and proliferation. [18] This pathway can also induce metastasis by regulating important steps like invasion and epithelial to mesenchymal transition (EMT). EMT is caused by a downregulation of E-cadherin. Examples of p38 pathway gene products that suppress E-cadherin are TWIST1 and SNAIL in mammary and ovarian cells respectively. [19] During EMT, normal polarized epithelial cells that attach to the basement membrane of the cell are changed into mesenchymal cells that are able to mobilize throughout the body and differentiate into other types of cells. [20] Invasion is also an important part of metastasis. The cells need to be able to move out of their primary tumor site and into distant tissues for optimal growth. The p38 pathway has numerous targets that can affect this phenotype; for example, the *LIMK1/2* genes are shown to be important in invasion in cSCC. [19,21]

1.4 LIMK2

The LIM kinase (LIMK) gene family consists of *LIMK1* and *LIMK2*. Both of these genes are important for metastasis and share very similar genomic structure. The LIMKs regulate actin rearrangement in a cell by phosphorylating cofilin which inactivates it. [22] Cofilin works as a depolymerization agent and the inactivation of cofilin causes a change in actin remodeling. The increase in actin remodeling can promote the formation of cell pseudopodia, a part of the cell used for movement. [23]

The LIMK family has multiple pathways which leads to its activation and subsequent contributions to metastasis. In vascular endothelial growth factor A (VEGF-A) induced cells, LIMK1 was activated by *MAPKAPK-2*, part of the p38 MAPK pathway. This activation led to actin reorganization and migration. [24] In colorectal cancer (CRC) cells, *LIMK2* was downregulated in more aggressive forms of CRC while *LIMK1* was upregulated. In this study, LIMK1 competed with LIMK2 to bind to beta-catenin in the Wnt/beta-catenin pathway. [25] Low expression of *LIMK2* in CRC also advanced EMT-induced metastasis. [25] In pancreatic cancer cells, *LIMK1* and *LIMK2* knockdowns caused a decrease in metastasis and angiogenesis. [26] In another study, LIMK2 was activated by ROCK which is a downstream protein of the Rho family GTPases. [27] LIMK and the MAPK pathway also share a common link in the p21 activated kinase (PAK). PAK phosphorylates LIMK to activate it which in turn leads to suppression of Cofilin. [28] PAK also activates the MAPK pathway by phosphorylating Raf1 and Nuclear factor-κB. [29] LIMK activation is a complex process mediated by

multiple pathways but its importance to cytoskeleton remodeling has been found in many cellular abnormalities, including cancer. This connection with the cytoskeleton and motility makes it an interesting variable in metastasis of cancer.

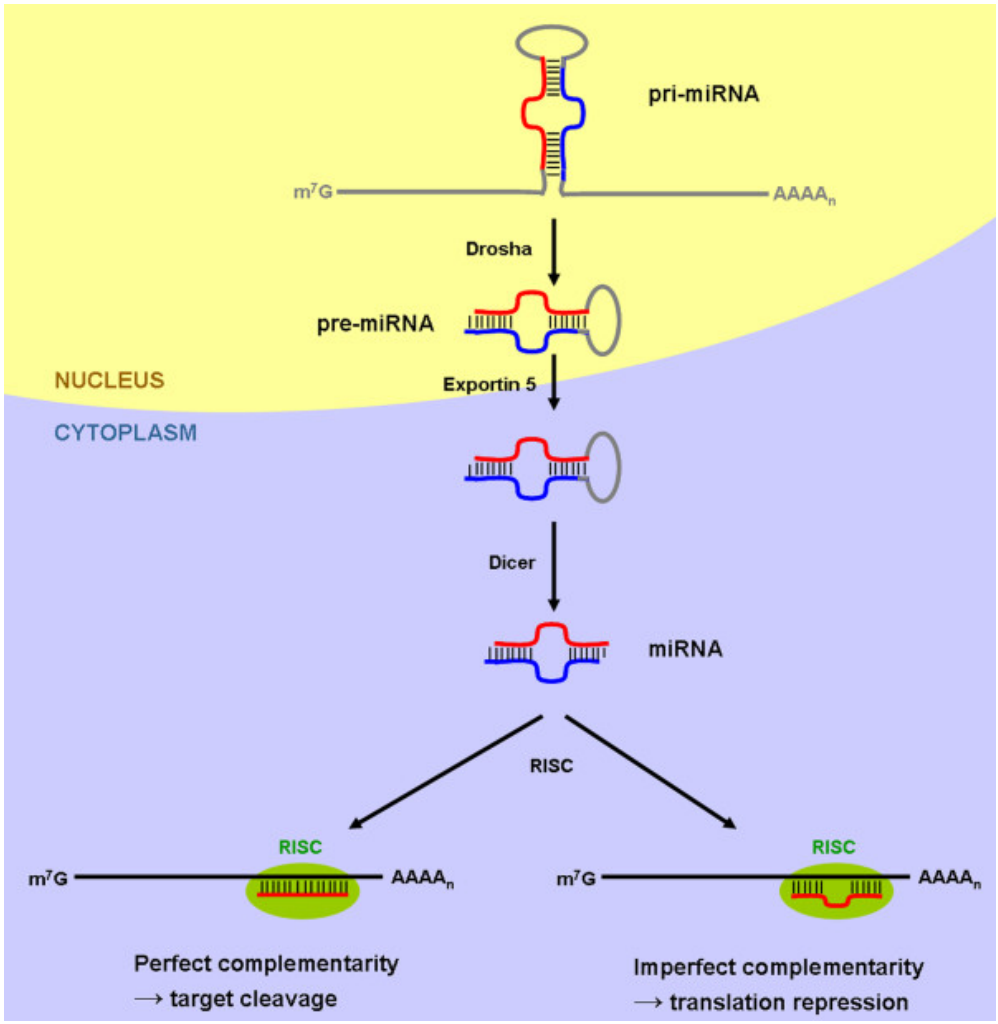

Figure 1: Canonical pathway of miRNA biogenesis. Adapted from Hoffman et al., 2012 [9] Pri-miRNAs are cleaved by Drosha enzyme to make pre-miRNA which is exported to cytoplasm. In cytoplasm, Dicer enzyme cleaves pre-miRNA into mature miRNA. Mature miRNA is loaded into miRNA-induced silencing complex (RISC) to target mRNA for degradation.

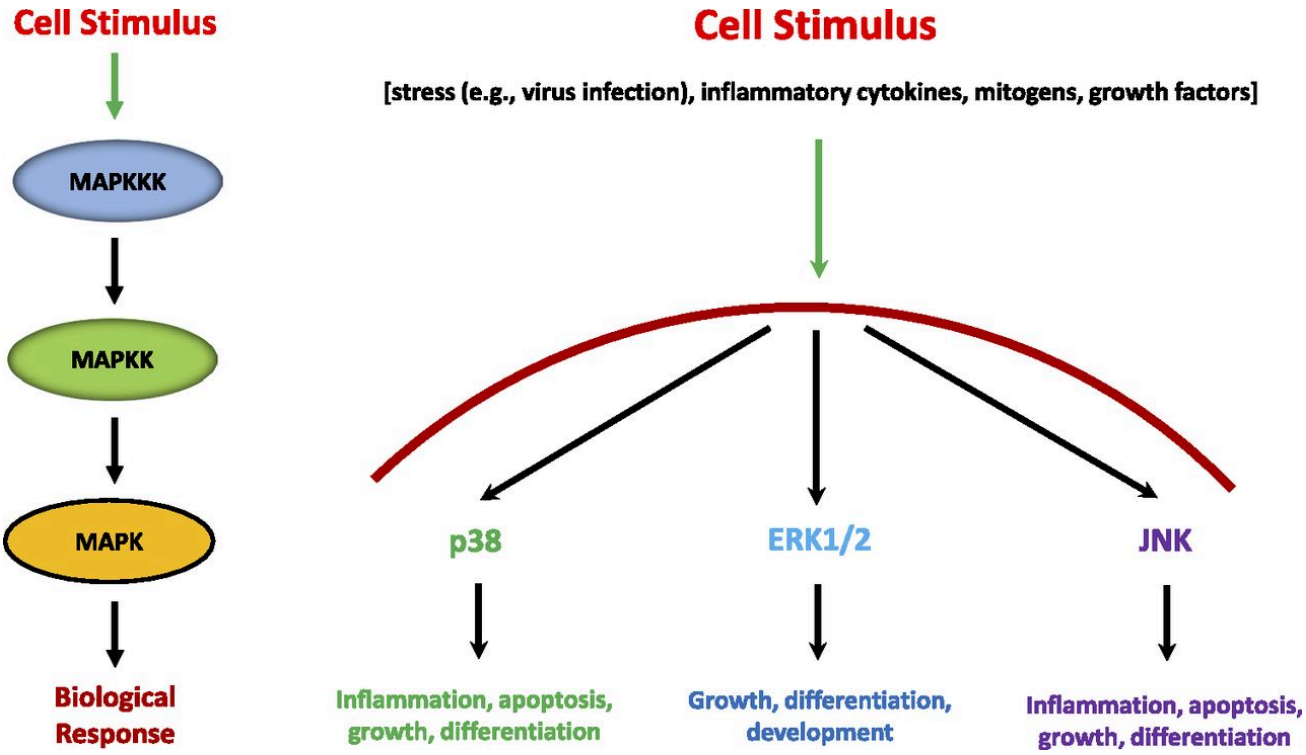

Figure 2. MAPK pathway and familial subsets. Adapted from Brutkiewicz, 2016 [18]. ERK1/2 is primarily stimulated by growth factors. JNK is stimulated by environmental stressors, inflammatory cytokines, and growth factors. P38 is primarily stimulated by environmental stress and inflammatory cytokines.

CHAPTER 2: BACKGROUND

2.1 Aggressive cSCC

Aggressive cutaneous squamous cell carcinoma (cSCC) metastasizes in 3.7-5.4% of cases. [30] Features that are associated aggressive tumors with a tendency to metastasize include certain anatomical locations, increased depth and diameter, presence of perineural invasion, poor differentiation, infiltrative growth pattern, and history of recurrence. [31] The ear and lip are locations that exhibit an increase in metastasis with one 1992 study showing metastatic rates of 11% and 13.7% respectively. [32] The same study found a 30.3% and 45.7% metastatic rate for tumors with diameters greater than 2 cm and depths greater than 4mm. [33] Approximately 32.8% of cSCCs that were poorly differentiated metastasized. [32] Finally, cSCCs with an infiltrative growth pattern had a 22.7% metastatic rate. [33] Only about 2-5% of cSCCs metastasize [34], but with over 700,000 new cases every year and over a 70% mortality rate of metastatic cSCC [6,35], it is imperative that aggressive cSCC is further studied in order to identify prognostic features and understand the metastatic process. A better understanding may lead to new therapeutic strategies targeting promoters of metastasis.

2.2 Previous Toland Lab Study

In a recently concluded project in the Toland lab, microRNA (miRNA) expression was evaluated in cSCCs isolated from sites associated with metastasis (aggressive sites), cSCCs at sites not associated with metastasis (non-aggressive sites), and non-tumor skin tissue. [36] The most common sites for primary cSCCs that become

metastatic cSCC are on the ear, lip, and temple. [1] Primary cSCCs at other sites, like limbs and the trunk, are less likely to metastasize. Of the 800 miRNAs profiled, approximately 150 miRNAs were expressed in tumor or skin samples in preliminary NanoString nCounter miRNA studies. Of the 150 miRNAs, 37 miRNAs showed at least a two-fold difference between tumor sites. Literature searches found that five of the miRNAs were found in cancer or diseases associated with the skin. Further analysis to validate five miRNAs of interest (miR-21-5p, miR-31-5p, miR-22-3p, miR-93-5p, and let-7g-5p) was done by quantitative real-time PCR (qRT-PCR) from the original 45 samples used for NanoString (18 aggressive sites, 15 non-aggressive sites, and 12 normal-adjacent skin) as well as previously isolated RNA from 30 additional tissue samples (7 aggressive sites, 14 non-aggressive sites, and 9 normal-adjacent skin). I conducted the validation of the 30 additional samples not used in the original studies. miR-21, miR-22, and miR-31 were upregulated in the aggressive tumor sites, with miR-21 and miR-31 showing statistically significant differences in expression when compared to normal tissue. These results were consistent with the preliminary NanoString nCounter boxplots (Figure 3). The upregulation of miR-31 from normal to aggressive sites of cSCC inspired my investigation into miR-31's role in metastasis (Figure 4).

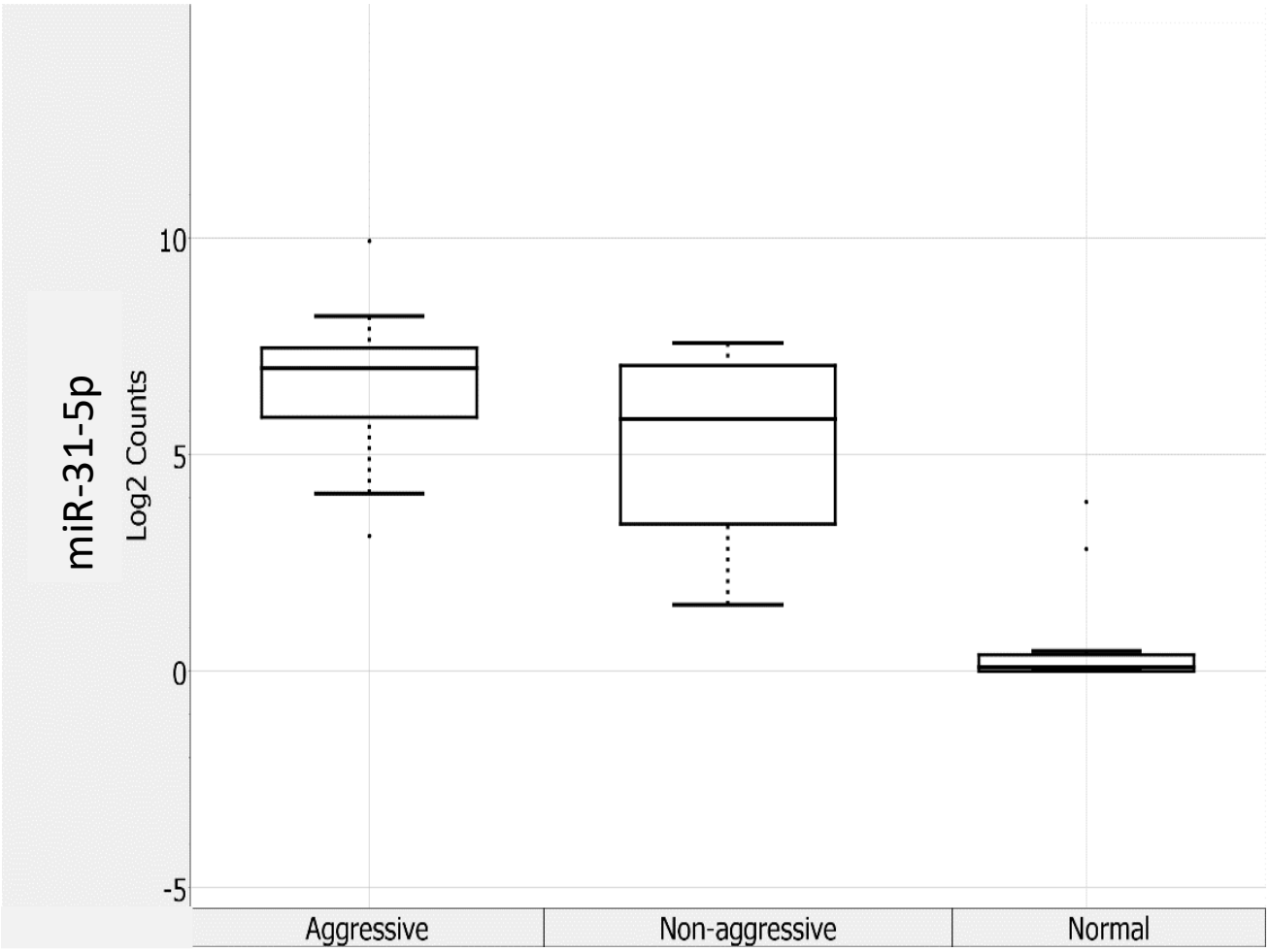

Figure 3: Box plot of miR-31-5p NanoString data. Box plot of miR-31 expression as measured by NanoString in the original samples shows highest expression in tumors from aggressive sites, followed by non-aggressive tumors and normal skin.

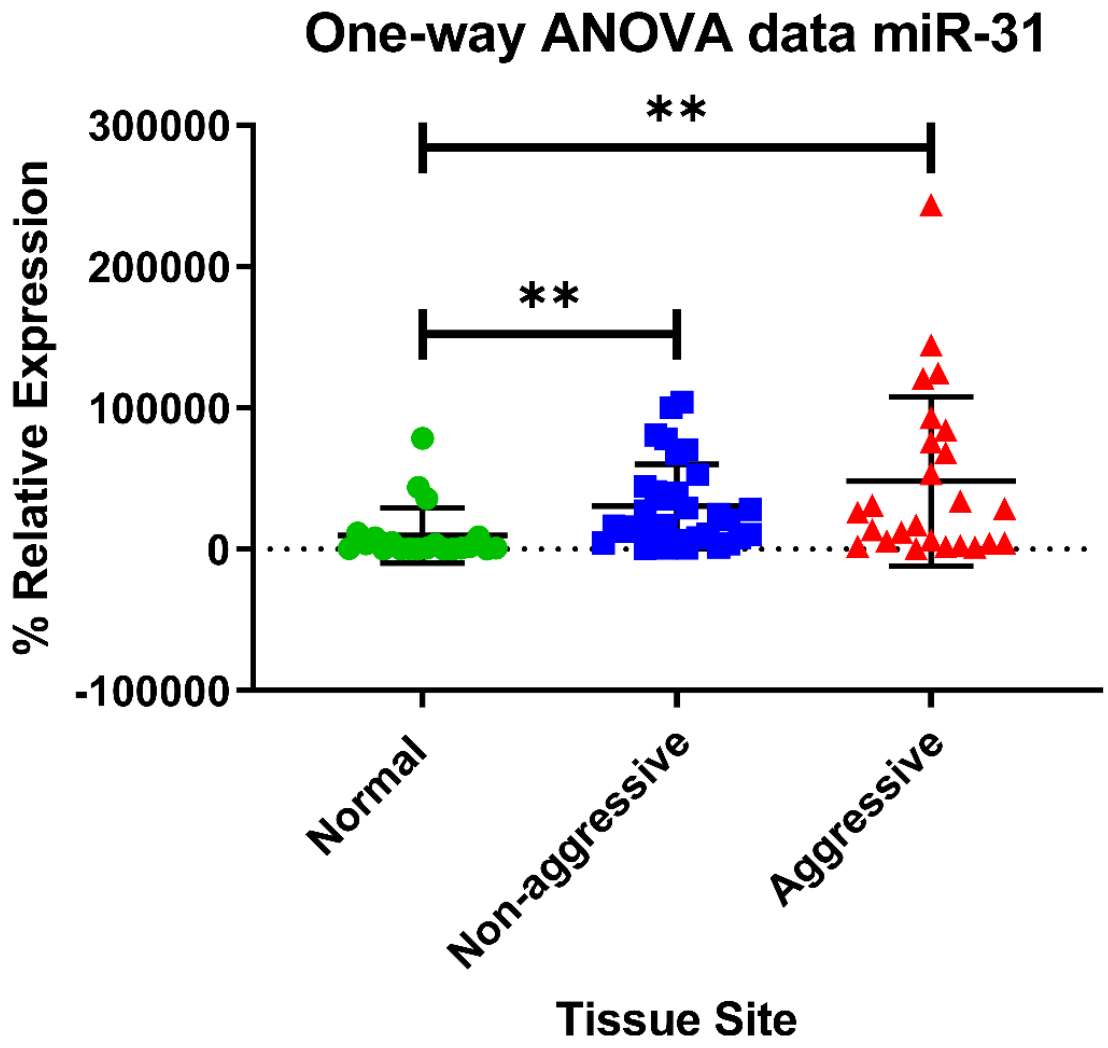

Figure 4: **One-way ANOVA of miR-31-5p in Toland Lab study.** One-way ANOVA data of miR-31 measured in normal skin, non-aggressive cSCC tumor sites, and aggressive cSCC tumor sites. n= 78. **= p-value < 0.01

CHAPTER 3: HYPOTHESIS AND SPECIFIC AIMS

The main hypothesis of this study is that miR-31 is important for cSCC metastasis. After a literature and database search of miR-31 targets, the hypothesis was refined to include that miR-31 regulates genes in the p38/MAPK pathway that are responsible for characteristics of metastasis like cell migration and invasion.

The specific aims of this study are stated below.

1. To determine if there is a link between increased miR-31 expression and metastatic phenotypes.
2. To determine if there is a link between miR-31 and genes expressed downstream of the p38/MAPK pathway.

CHAPTER 4: MATERIALS AND METHODS

4.1 HaCaT and SRB-12 cell lines

HaCaT is a human immortalized keratinocyte cell line used to mimic normal cells. SRB-12 is a cutaneous squamous cell carcinoma cell line derived from a human cSCC. Cell lines were tested for mycoplasma using the manufacturer's protocol from the LookOut® Mycoplasma PCR Detection Kit (Sigma-Aldrich). Cell line identity was validated using the cell line authentication service of the OSU Genomics Shared Resource. HaCaT cells were grown in Dublecco's Modified Eagle Medium (DMEM, Gibco) supplemented with 15% fetal bovine serum (FBS, Sigma), 1% penicillin streptomycin (Corning), and 1% sodium pyruvate (Sigma). SRB-12 cells were grown in DMEM/F12 (1:1, Gibco) supplemented with 10% FBS and 1% penicillin streptomycin.

4.2 Transfection

In 24-well plates (1.9 cm^2), HaCaT cells were plated with 200,000 cells per well and SRB-12 cells were plated with 150,000 cells per well one day prior to transfection. All transfections were done using Lipofectamine RNAiMAX. miR-31 was introduced to cells by transfection of hsa-miR-31 mirVana miRNA mimic and miR-31-3p expression was reduced using Anti-miR-31 miRNA inhibitor (Ambion). According to the manufacturer's RNAi Transfection protocol, 50 µl of miRNA-lipid complex was added to a final volume of 500 µl per well. Cells were harvested one day after transfection.

4.3 Identification of Genes of Interest and Primer Design

Through database searches of miR-31, possible targets of miR-31 were identified. The databases used were miRWalk 3.0, miRDB, and Target Scan 7.0. Additional literature

searches led to the formation of the preliminary list of genes that were examined in this project. Those genes included: *MAPKAPK2, DUSP7, STAT3, MAP3K1, MAPK14, MAP2K4, MEF2A, CREB1,* and *LIMK2.* The genes chosen were either included in the p38/MAPK pathway or were related to the pathway. The role of p38/MAPK in metastatic phenotypes made this pathway of particular interest. [16,19] The common link of UV radiation activating the p38/MAPK pathway and playing an important role in cutaneous squamous cell carcinoma also sparked inquiry into the connection between cSCC metastasis, the p38/MAPK pathway, and miR-31. [1,5,17]

SYBR Green Primers for qRT-PCR were designed based on previous primers found in literature (Table 1). [37-45]

4.4 Quantitative Real-Time PCR

RNA was extracted from transfected cells using RiboZol RNA Extraction Reagent (Amresco) according to the manufacturer's recommended protocols. cDNA for qRT-PCR of target genes of interest was made using 1ug of RNA and the iScript cDNA Synthesis Kit (BioRad). cDNA for miR-31 was made using TaqMan Advanced miRNA Assays kits (ThermoFisher). miR-31 expression was normalized using *RNU6B*, a low-expressed reference gene. Relative Quantification Fast SYBR Green qPCR was used to measure the candidate miR-31 target genes of interest: *LIMK2, MAPKAPK2, DUSP7, STAT3, MAP3K1, MAPK14, MAP2K4, MEF2A,* and *CREB1*. *GAPDH* was used to normalize for gene expression. Relative Quantification Fast TaqMan qPCR was used to evaluate the impact of miR-31 on genes of interest, *LIMK2, MEF2A,* and *DUSP7* with PrimeTime Standard qPCR 5' FAM 3' ZEN™/Iowa Black® nuclease assays (Integrated DNA Technologies). *HPRT1* was used to normalize TaqMan data. A no-RT control was

used for each sample and a no template control was used for each primer. 5 µL PrimeTime™ Gene Expression 2X Fast Master Mix (Integrated DNA Technologies), 2.5 µL of cDNA, and 2.5 µL probe mix was used for each 10 µL qRT-PCR reaction a 384 well plate. All qPCR was performed in triplicate. Samples were processed by the OSU Genomics Shared Resource.

The gene expression relative to the control gene was quantified using the formula: $2^{\Delta Ct}$*100. ΔCt was calculated by control gene expression-target gene expression.

4.5 Proliferation Assay

The MTT ((3-(4,5-Dimethylthiazol-2-yl)-2,5-diphenyltetrazolium bromide) Cell Proliferation Kit I and procedure (Roche) was used to measure cell proliferation in HaCaT cells. One day post-transfection with miR-31 mimic or inhibitor, cells were harvested using 0.25% trypsin (Corning), manually counted using trypan blue and a hemocytometer, and plated in quadruplicate in a 96 well plate with 4,000 cells per well. After a 24-hour incubation period, the kit's MTT labeling reagent was added and the cells were incubated for an additional 4 hours. The solubilization agent was added and after overnight incubation, absorbance at 550nm and 670nm was recorded on a spectrophotometer. 0, 24, and 48 hour post incubation with MTT time points were recorded. Cells were incubated at 37°C and 5% CO_2 throughout the assay.

MTT data was analyzed by A_{550nm} – reference A_{670nm}. The average blank absorbance was subtracted from the $A_{550nm} – A_{670nm}$ value. These values were then averaged across the four wells per sample. Fold change was determined by dividing average value for each variable at 24 or 48 hours by the average value at hour 0.

4.6 Western Blot Analysis

HaCaT cells were harvested 24 hours post-transfection and protein was extracted using a 1:25 solution of 25X protease inhibitor and RIPA buffer. Thirty µg of protein was run on 10% SDS-PAGE gels by electrophoresis for 90 minutes at 150 volts in 1x Running Buffer (25 mM Tris Base, 38 mM glycine, 0.1% SDS, ddH_2O). Protein was transferred to nitrocellulose membranes, (GE Healthcare Life Sciences) at 90 volts for 70 minutes in 1x Transfer Buffer (25 mM Tris Base, 190 mM glycine, ddH_2O). The membrane was blocked in 5% milk in TBST (phosphate-buffered saline with 0.01% Tween 20) for 1 hour. A 1:1000 dilution of the primary antibody in 5% milk in TBST was added to the membrane and incubated at 4°C overnight. Three 15 min TBST washes were done, followed by a 2 hour incubation with secondary antibody at room temperature. A 1:5000 anti-rabbit secondary antibody (GE Healthcare UK Limited, NA934V) was used for phoso-CREB (Cell Signaling Technology, 9198) and p44/42 MAPK primary antibodies (Cell Signaling Technology, 9102). A 1:1000 anti-mouse secondary antibody (Jackson ImmunoResearch Laboratories, 115-035-003) was used for the STAT3 primary antibody (Cell Signaling Technology, 9139). GAPDH was used as a loading control (Santa Cruz Biotechnology, 25778). Following three washes, the SuperSignal West Pico Chemiluminescent Subrate Kit (ThermoFisher) was used to help visualize the western blot in a LI-COR Odyssey Fc Imager. Image analysis was performed in ImageJ.

4.7 Migration Assay

Migration Assays were performed with the HaCaT and SRB-12 cell lines. Cells transfected with miR-31 mimic and miR-31 inhibitor were harvested from 24-well plates at 24 hours post-transfection. Seventy µL of cells in 1% FBS media was added to each

well in a 2 well Culture-Insert (ibidi) placed in a 35mm x 10 mm culture dish. HaCaT cells were plated at 100,000 per well and SRB-12 cells were plated at 75,000 cells per well. The Culture-Insert was removed 24 hours later. Pictures were taken under a Fluorescent Cell Imager every 4 hours. Cells were incubated at 37°C and 5% CO_2 throughout the assay. Each variable was tested in duplicate and the experiment was repeated 3 times per cell line.

Table 1. Published SYBR Green primers for candidate mir-31 target genes.

Gene	SYBR Green Primer
LIMK[37]	Forward: 5′-GGGGCATCATCAAGAGCA-3′ Reverse: 5’-GAGGACTAGGGTGGTTCAG-3’
MAPKAPK2[38]	Forward: 5’-CAGCAGTTCCCGCAGTTC-3’ Reverse: 5’-CGAATTTCTCCTGGGTCCTC-3’
DUSP7[39]	Forward:5′–TCATTGACGAAGCCCG–3′ Reverse:5′–GCGTATTGAGTGGGAACA–3′
STAT3[40]	Forward: 5’ -GCTTTTGTCAGCGATGGAGT-3’ Reverse: 5’ -ATTTGTTGACGGGTCTGAAGTT-3’
MAP3K1[41]	Forward: 5’-CACGAATGGTTGGAAAGGAGAA-3’ Reverse:5’-AGATCCATCTCCTTTAACTGGGATT-3’
MAPK14[42]	Forward: 5’-GAGAGGCCCACGTTCTACC-3’ Reverse: 5’-CGTAACCCCGTTTTTGTGTCA-3’
MAP2K4[43]	Forward:5′-GATGAATCCAAAAGGCCAAA-3′ Reverse:5′-TCAATCGACATACATGGGAGAG-3′
MEF2A[44]	Forward: 5’-TCAAGCCACACAACCTCTTG-3’ Reverse: 5’-CAGCATTCCAGGGGAAGTAA-3’
CREB1[45]	Forward: 5’-GCTGCCTCTGGAGACGTACAA-3’ Reverse: 5’-GCTAGTGGGTGCTGTGCGA-3’

CHAPTER 5: RESULTS

5.1 miR-31 is upregulated in SRB-12 and COLO-16 compared to HaCaT

To determine the level of expression of miR-31 in 3 human skin cell lines, RT-qPCR was performed. miR-31 expression was measured in HaCaT- an immortalized human kertatinocyte cell line, SRB-12- a human cSCC cell line, and COLO-16- a human cSCC cell line. There was a 3.0-fold change in miR-31 expression between HaCaT and COLO-16 cell lines (p-value=0.0078). There was a 2.6-fold difference in expression between SRB-12 and HaCaT cells, but this was not statistically significant (p-value=0.06) (Figure 5). The higher expression of miR-31 in cSCC cells indicates that it plays a role in cancer phenotypes.

5.2 miR-31 has multiple target genes that are associated with p38/MAPK pathway

Gene targets of miR-31-5p were identified using the following miRNA databases: miRWalk 3.0, miRDB, and Target Scan 7.0. miR-31 targets were narrowed down by literature search looking for genes with expression in skin and association with the p38/MAPK pathway. *MAPKAPK2, DUSP7, STAT3, MAP3K1, MAPK14, MAP2K4, MEF2A, CREB1, and LIMK2* were the genes chosen to be investigated. [24, 46-54] (Table 2)

5.3 Multiple genes of interest show no trends in HaCaT cells transfected with miR-31 mimic and inhibitor

To investigate role of miR-31 in regulating target genes of interest, i.e. *MAPKAPK2, DUSP7, STAT3, MAP3K1, MAPK14, MAP2K4, MEF2A, LIMK2, and CREB1*, SYBR Green primers targeting the genes were first tested on cDNA from HaCaT, SRB-12, and

COLO-16 cells. The *LIMK2, MEF2A*, and *DUSP7* SYBR Green primers failed to generate clean SYBR green dissociation curves or to result in detectable product; thus, TaqMan PrimeTime nuclease assays of these 3 genes were used for subsequent qPCR analysis.

HaCaT cells were transfected with miR-31 mimic, anti-miR-31 inhibitor, a mock control, and a no transfection control. RNA was harvested at 24, 48, and 72 hours. miR-31 expression was measured to test the efficiency of each transfection before measuring gene expression (Figure 6A,B). SYBR Green qPCR was used to measure the expression of these initial genes of interest. Genes *MAPKAPK2, STAT3, MAP3K1, MAPK14, MAP2K4, and CREB1* showed no trend or significant difference between transfections (Figure 7A-F). This indicates that these genes are not regulated by miR-31.

TaqMan qPCR was used to test level of expression of genes *LIMK2, MEF2A*, and *DUSP7* in HaCaT cells. HaCaT cells were transfected with miR-31 mimic, miR-31 inhibitor, a mock control, or a no transfection control. RNA was harvested at 24, 48, and 72 hours post-transfection. *DUSP7* showed no trend or significant difference between transfections (Figure 8A). *LIMK2* and *MEF2A* showed trends of cells transfected with miR-31 mimic having lower gene expression than cells transfected with anti-miR-31 inhibitor (Figure 8B,C). *MEF2A* had a non-significant 1.3-fold decrease between miR-31 and anti-miR-31 at 48-hours post-transfection. *LIMK2* had a non-significant 1.3-fold decrease between miR-31 and anti-miR-31 in the 24-hour transfection and a non-significant 1.6-fold decrease in the 48-hour transfection. A second experiment showed a

similar trend of decreased of *LIMK2* in HaCaT cells transfected with miR-31 mimic, miR-31 inhibitor, a mock control, and a no transfection control at 24 and 48 hours.

5.4 LIMK2 expression is downregulated in HaCaT cells transfected with miR-31

LIMK2 expression was measured by qPCR in HaCaT cells transfected with miR-31 mimic, miR-31 inhibitor, a mock control, or a no transfection control. Expression was measured relative to a *HPRT1* control. After two qPCR experiments, a non-significant trend of lower *LIMK2* expression was observed in the miR-31 transfected cells relative to the anti-miR-31 transfected cells with a 1.7-fold change. A third experimental run showed a change in trend with higher *LIMK2* expression in the miR-31 transfected cells relative to the anti-miR-31 HaCaT cells. An average of the three qPCR plates showed a 1.2-fold increase in *LIMK2* in the anti-miR-31 cells compared to the miR-31 in the 24-hour transfection. There was no fold change between miR-31 and anti-miR-31 transfected cells in the 48-hour HaCaT transfection (Figure 9). When combining data across experimental plates, there was not a significant decrease in *LIMK2* expression in the miR-31 transfected cells.

5.5 STAT3 protein expression is upregulated in miR-31 transfected HaCaT cells

To test for translational effects of genes related to the MAPK pathway, western blot analysis was conducted on HaCaT cells 24-hours post-transfection. HaCaT cells were transfected with miR-31 mimic, anti-miR-31 inhibitor, mock, or no transfection controls. STAT3, phoso-CREB, and p44/42 MAPK antibodies were used to measure protein expression in these cells. Phospho-CREB showed no detectable expression. STAT3 protein was upregulated 2.1-fold and 3.3-fold in miR-31 transfected cells compared to anti-miR-31 and mock transfected cells, respectively (Figure 10). p44/42 MAPK

expression showed no significant differences between transfection types (Figure 11). All quantification of staining was done in ImageJ. As upregulation is not expected for a direct microRNA target, no additional experiments were done looking at STAT3.

5.6 miR-31 has no effect on cell proliferation in HaCaT cells

To determine the effects of miR-31 on cell proliferation, HaCaT cells were transfected with miR-31 mimic, anti-miR-31 inhibitor, mock, or no transfection controls. Proliferation was measured at 0, 24, and 48 hour post-transfection time points via an MTT assay. There was a significant difference between the optical density in miR-31 mimic and mock (p-value<0.0001) and miR-31 mimic and no transfection wells (p-value=0.0002) at hour 48 (Figure 12). There was no significant difference between miR-31 mimic and anti-miR-31 transfected cells. miR-31 transfected cells exhibited a 3.2-fold change between 0 and 48 hours. Anti-miR-31 transfected cells exhibited a 4.1-fold change between hour 0 and 48. Mock transfected cells showed a 4.5-fold change between 0 and 48 hours. No transfection control cells had a 4.6-fold change between hour 0 and 48. These results suggest that miR-31 does not play a role in cell proliferation.

5.7 miR-31 does not regulate *LIMK2* expression in SRB-12 cells

After establishing a possible association of *LIMK2* with miR-31 in HaCaT cells, *LIMK2* expression was measured in cSCC SRB-12 cells transfected with miR-31 mimic, anti-miR-31 inhibitor, mock, or no transfection controls. *LIMK2* expression was measured by qPCR 24-hours and 48-hours post-transfection. Each transfection and qPCR quantification was performed in triplicate. There was no significant difference between

transfection types (Figure 13). These results suggest that miR-31 does not regulate *LIMK2* mRNA levels in SRB-12 cells.

5.8 miR-31 promotes cell migration

To determine if miR-31 affects cell migration, HaCaT and SRB-12 cell lines were transfected with miR-31 mimic, anti-miR-31 inhibitor, or mock. 24-hours post-transfection cells were placed in a 2 well Culture-Insert and subjected to a migration assay. Twenty-four hours after placing the cells, the insert was removed and closure of the gap left from the insert was observed over a 24-hour period. HaCaT cells exhibited the most gap closure in miR-31 mimic transfected cells at the end of the 24-hour period (Figure 14). They also showed the most closure at the 8-hour time point. In HaCaT cells, the anti-miR-31 transfected cells displayed the least amount of closure after 24 hours. Mock cells had an intermediate amount of closure (Figure 14). SRB-12 miR-31 mimic transfected cells also showed more closure after 24 hours, although not as much as HaCaT cells. Mock and anti-miR-31 transfected cells showed similar amounts of closure at the 8 and 24-hour time points (Figure 15).

Table 2: Gene targets of miR-31-5p and their role in p38/MAPK pathway

Target	# target sites in 3' UTR- *Homo sapiens*	Role
LIMK2	1	Activated by *MAPKAPK2* to phosphorylate *ANXA1*[46]; forms lamellipodia for cell migration[24]
MAPKAPK2	1	P38 activates/ phosphorylates gene to phosphorylate HSP27 which has a role in inhibition of apoptosis and actin cytoskeletal remodeling[47]
DUSP7	2	dual-specificity protein phosphatase, DUSP inactivates p38 dephosphorylates activation loop, chosen because high in skin[48]
STAT3	1	Transcription factor activated by p38, regulates cell growth, apoptosis, immune response, and DNA damage response[49]
MAP3K1	1	Regulates cell migration and pro-survival signaling, loss of gene expression reduces cell migration and invasion and delays metastasis[50]
MAPK14	2	Another name for p38α, activated by environmental stress and pro-inflammatory cytokines, regulates cell proliferation, differentiation, migration, and survival[51]
MAP2K4	1	Tumor suppressing gene[52]
MEF2A	0 (1 in coding region)	Found in molecular mechanisms of cancer, actin cytoskeletal signaling[53]
CREB1	0 (1 in 5'UTR 1 in coding region	Phosphorylated by *MAPKAPK2*[54]

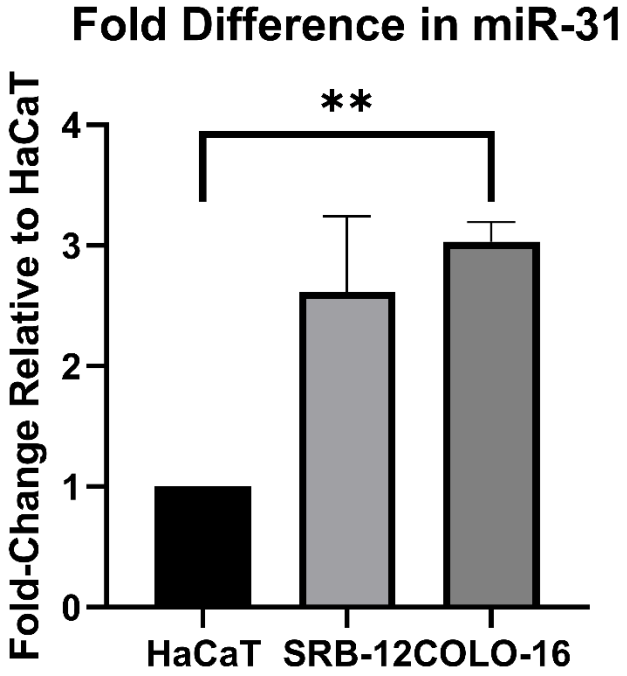

Figure 5: Fold difference in miR-31 expression between HaCaT, SRB-12, and COLO-16 cell lines. miR-31 was upregulated in SRB-12 2.6-fold compared to HaCaT (p-value=0.06). A significant difference in expression between HaCaT and COLO-16 was observed. **=p-value<0.01

A

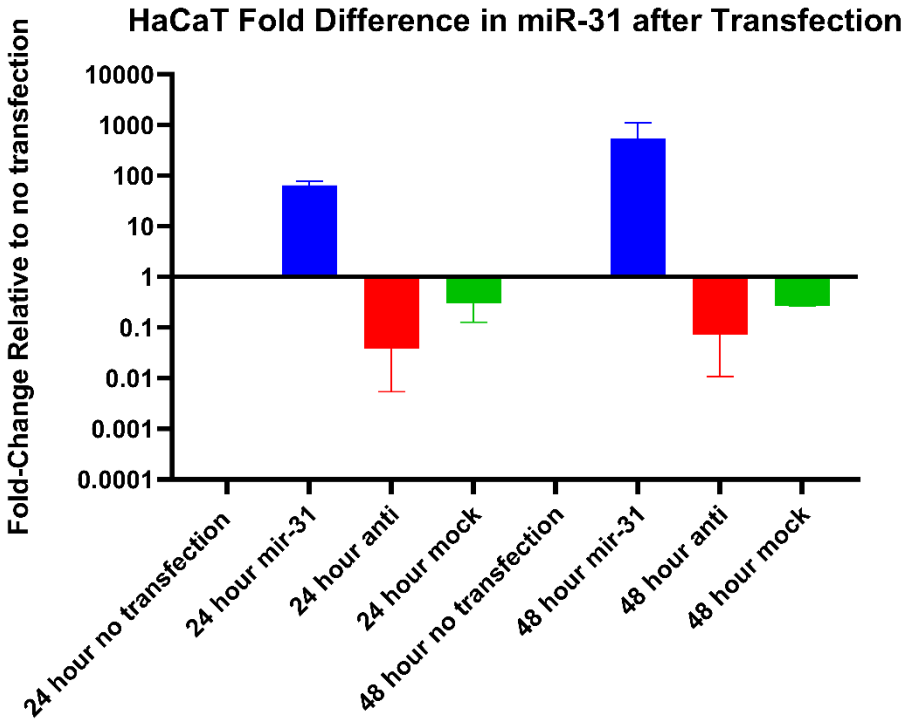

B

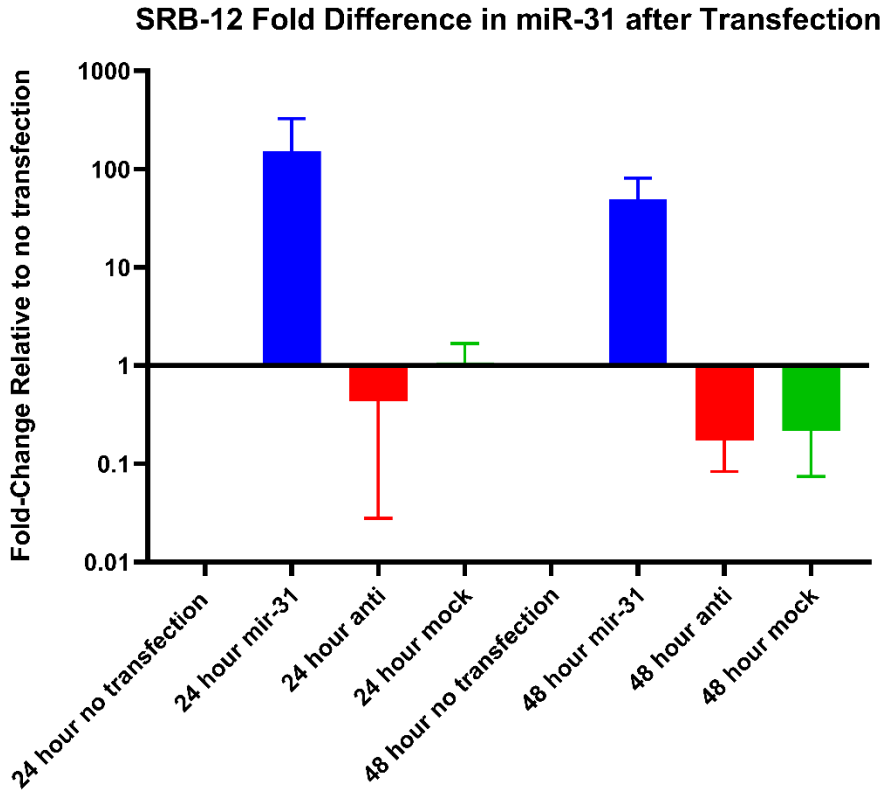

Figure 6: miR-31 expression post-transfection. HaCaT (A) and SRB-12 (B) cells were transfected with miR-31 mimic (blue), anti-miR-31 inhibitor (red), mock (green), or no transfection (purple) prior to functional studies. miR-31 expression was measured 24 and 48 hours post-transfection. *RNU6B* was used as a loading control to normalize between samples. Fold-change was found relative to no transfection, which is plotted on the graph at 1. A representative result is shown.

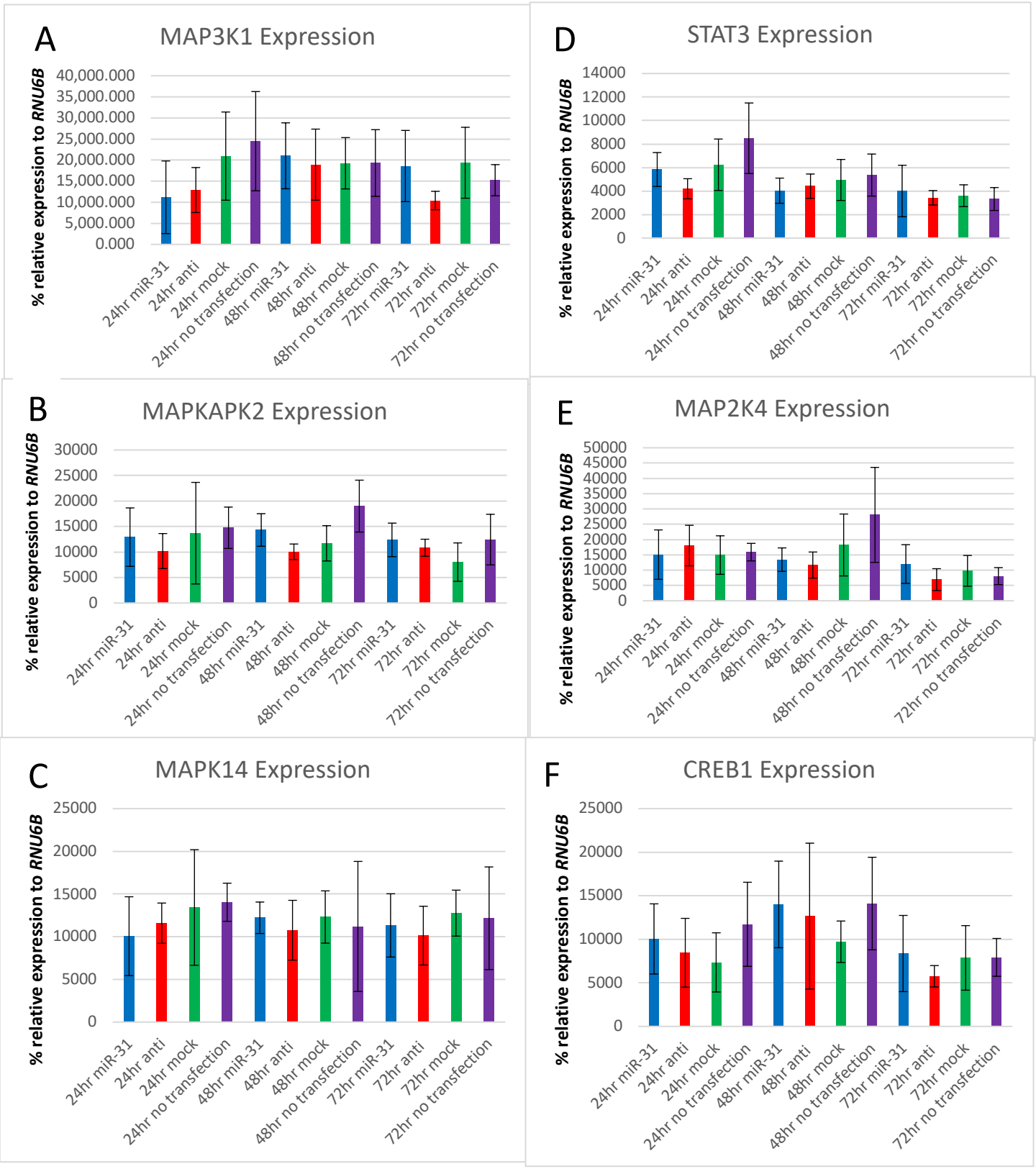

Figure 7: **qPCR results from genes tested with SYBR Green primers**. HaCaT cells were transfected with miR-31 mimic (blue), anti-miR-31 inhibitor (red), mock (green), and no transfection (purple). Gene expression was measured at 24, 48, and 72-hours post-transfection. *MAP3K1* (A), *MAPKAPK2* (B), *MAPK14* (C), *STAT3* (D), *MAP2K4* (E), and *CREB1* (F) showed no consistent trend amongst time points and did not display the expected lower expression in miR-31 mimic transfected cells. *GAPDH* was used as a control to normalize expression between samples.

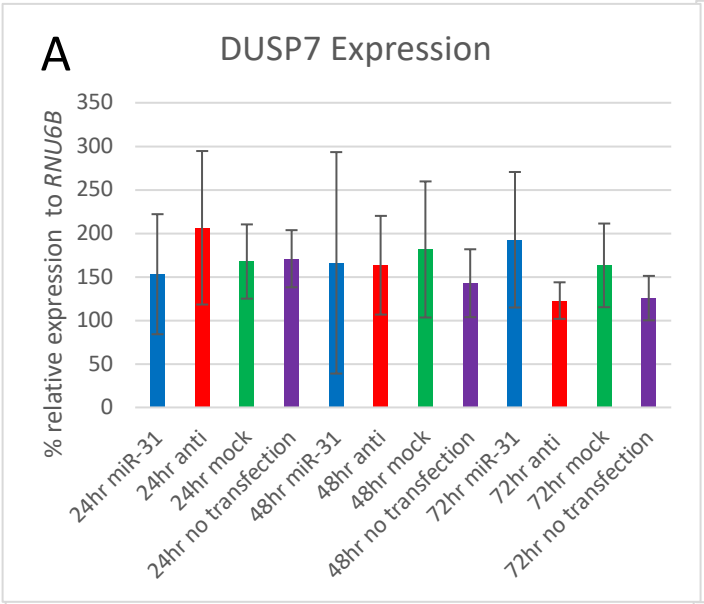

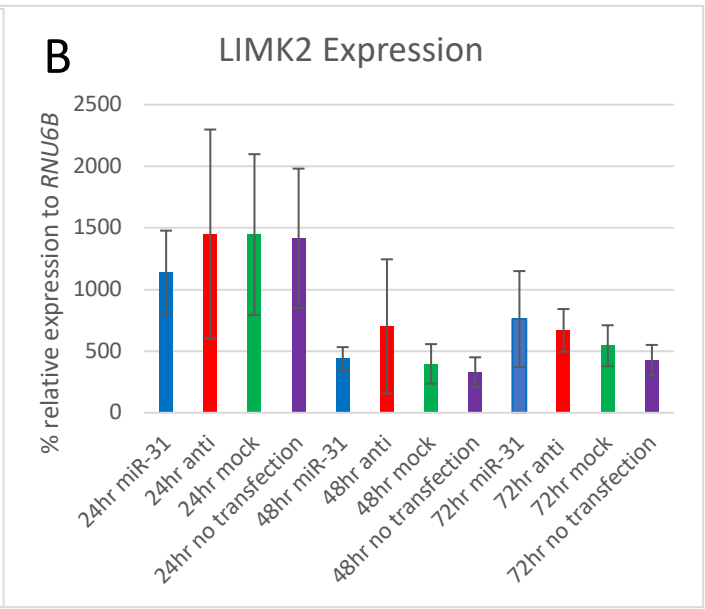

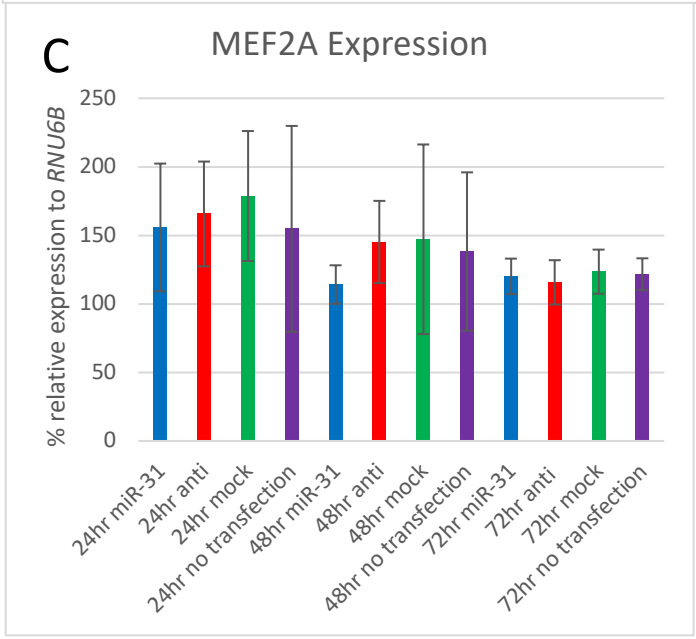

Figure 8: **qPCR results from genes tested with PrimeTime TaqMan Primers.** HaCaT cells were transfected with miR-31 mimic (blue), anti-miR-31 inhibitor (red), mock (green), or no transfection (purple). Gene expression was measured at 24, 48, and 72-hours post-transfection. *DUSP7* (A) showed no trend or significance between transfection types. *LIMK2* (B) and *MEF2A* (C) showed non-significant trends of cells transfected with miR-31 mimic having lower gene expression than cells transfected with anti-miR-31 inhibitor. These results were relatively consistent between the 24 and 48-hour time points. *HPRT1* was used as a control to normalize gene expression between samples.

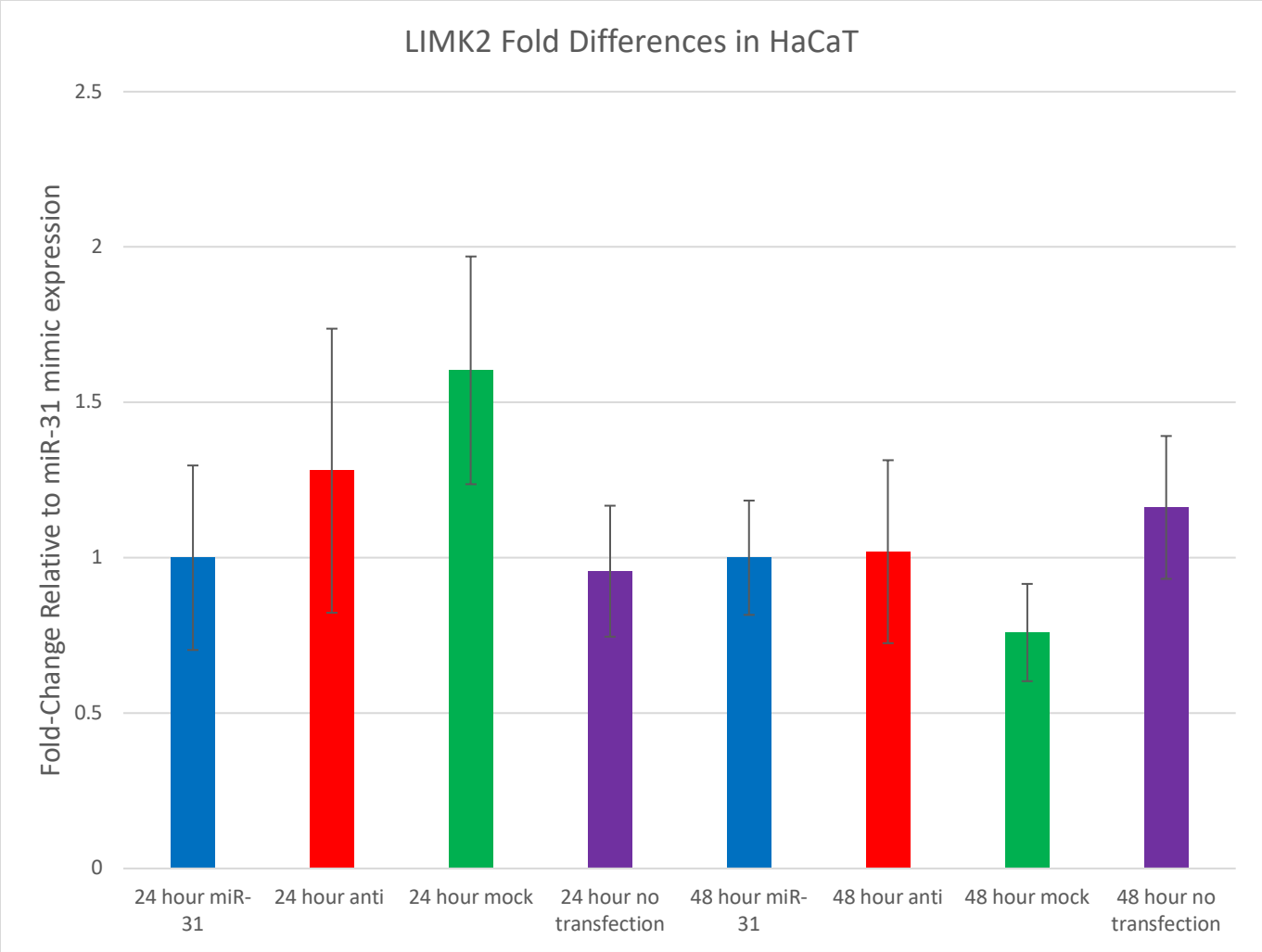

Figure 9: Fold differences in *LIMK2* expression for HaCaT. *LIMK2* expression was measured by qPCR in HaCaT cells transfected with miR-31 mimic (blue), anti-miR-31 (red), mock (green) or no transfection (purple) 24- and 48-hours post-transfection. *HPRT1* was used to normalize for expression. There was no significant difference between transfection types. qPCR was performed in triplicate; results shown are the average fold-change across three plates.

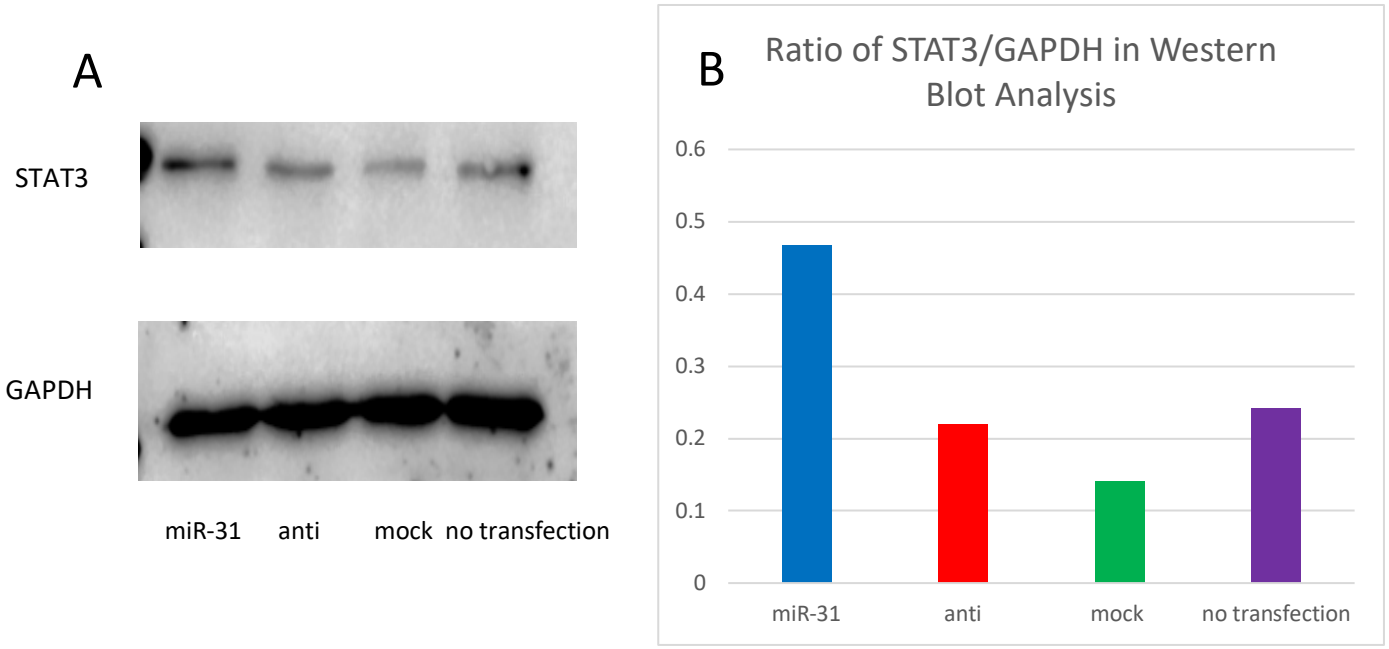

Figure 10: STAT3 is upregulated in miR-31 mimic transfected HaCaT cells. A. Western blot image taken in a LI-COR Odyssey Fc Imager. B. STAT3 was upregulated 2.1-fold in miR-31 mimic transfected cells compared to anti-miR-31 transfected cells and 3.3-fold compared to mock transfected cells. Bands were quantified in ImageJ.

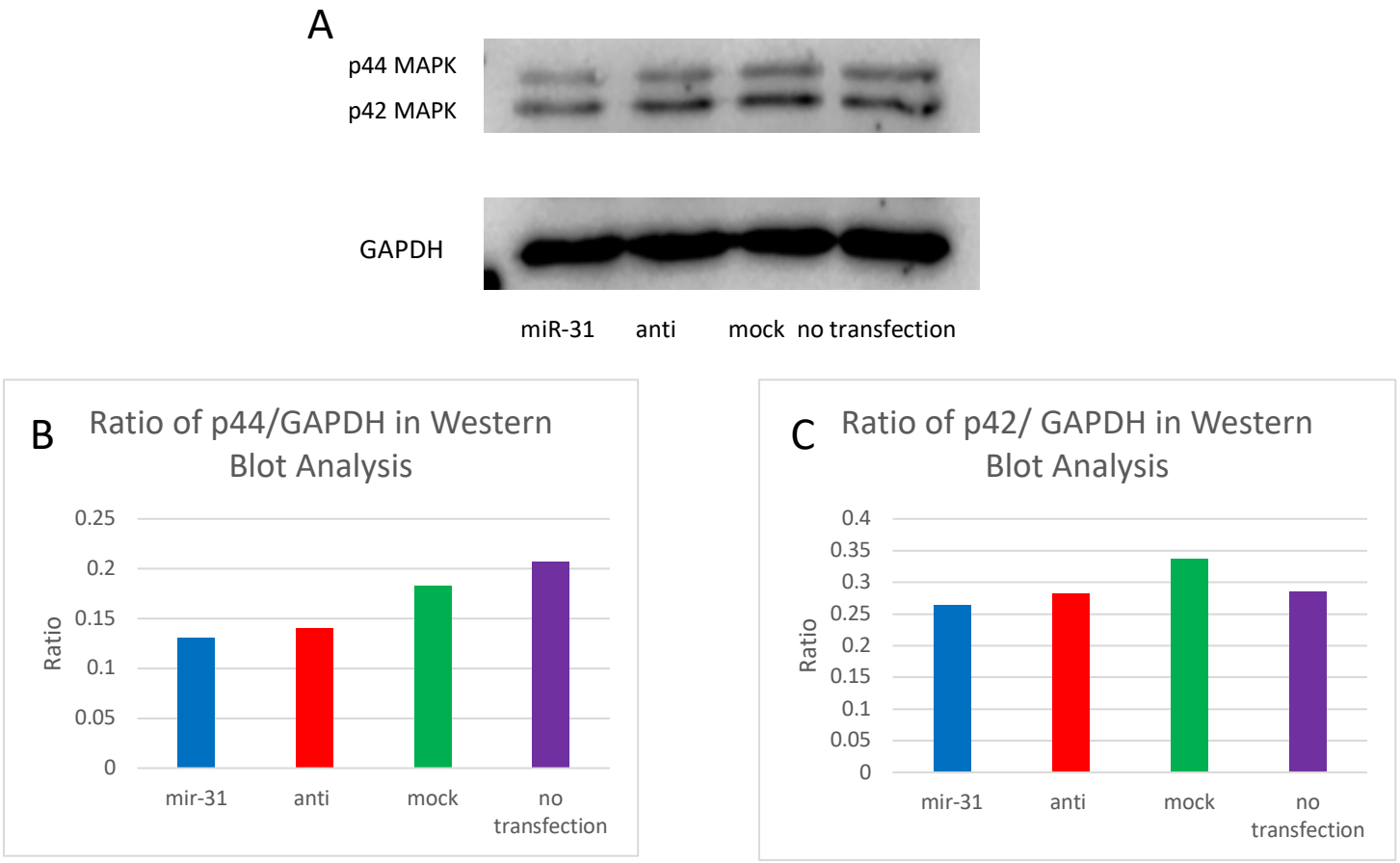

Figure 11: p44/42 MAPK showed no difference between transfection types. (A) miR-31 mimic, anti-miR-31 inhibitor, mock, or no transfection HaCaT cells showed no significant difference in p44/42 MAPK protein expression as measured by western. There was slightly higher expression of p42 (B) compared to p44 (C) after normalization to GAPDH expression in all transfection types. Quantification of bands was done in ImageJ.

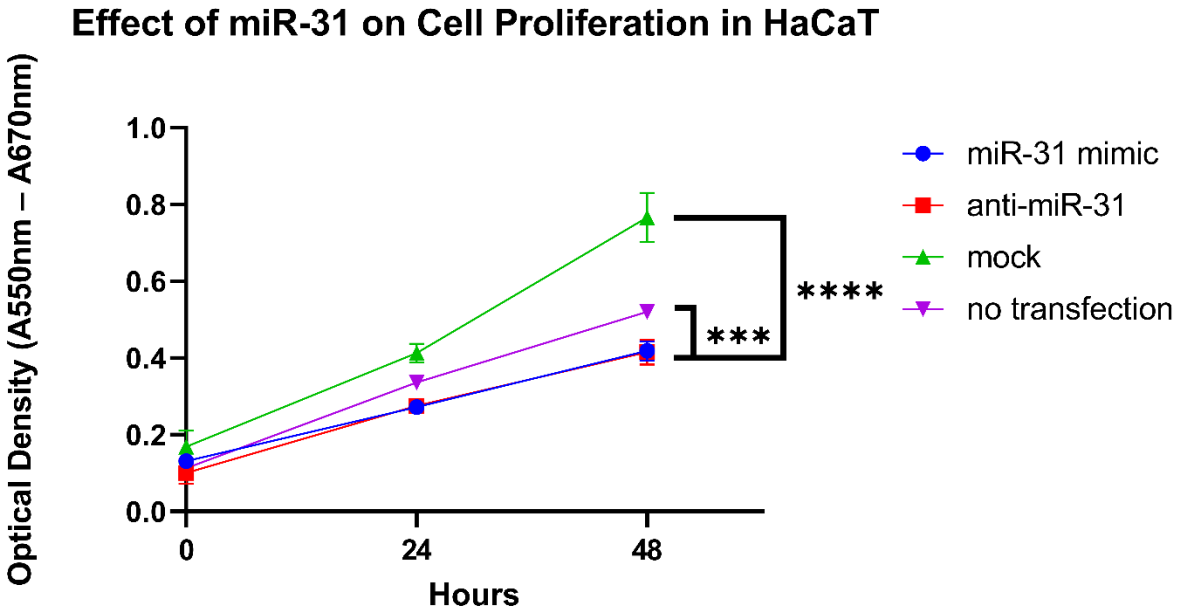

Figure 12: **Effect of miR-31 on cell proliferation**. Cell Proliferation was measured at 0, 24, and 48 hours after transfection in HaCaT cells transfected with miR-31 mimic (blue circle), anti-miR-31 (red square), mock (green upright triangle), or no transfection (purple downward triangle). At 48 hours, there was a significant difference between miR-31 and mock (p-value<0.0001) and miR-31 and no transfection (p-value=0.0002). Proliferation was measured in quadruplicate at each time point. ***=p-value<0.001, ****=p-value<0.0001

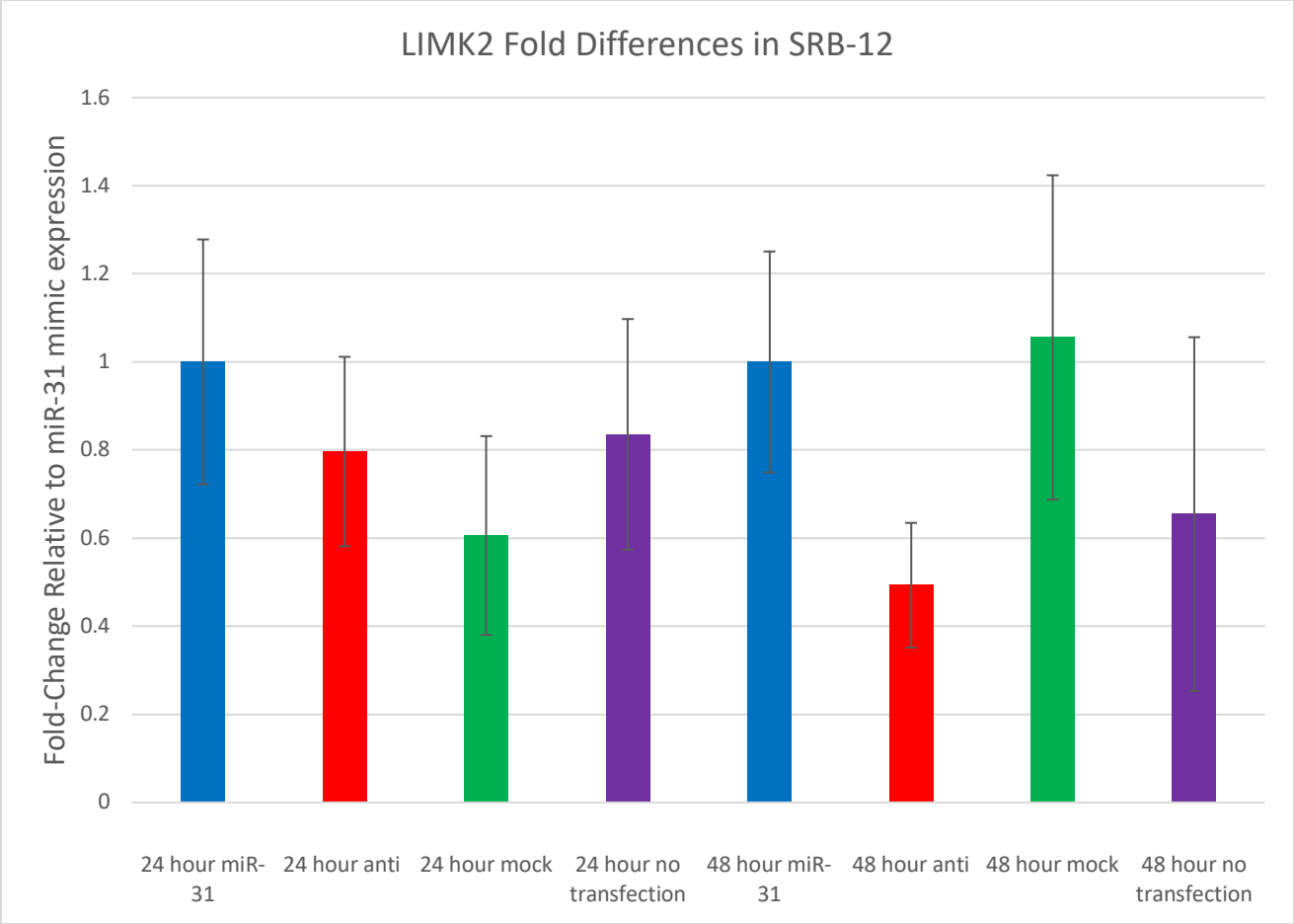

Figure 13: Fold differences in *LIMK2* expression for SRB-12. *LIMK2* expression was measured by qPCR in SRB-12 cells transfected with miR-31 mimic (blue), anti-miR-31 (red), mock (green), or no transfection (purple) 24 and 48 hours post-transfection. *HPRT1* was used to normalize for expression. There was no significant difference between transfection types. qPCR was performed in triplicate; results shown are the average fold-change across three plates.

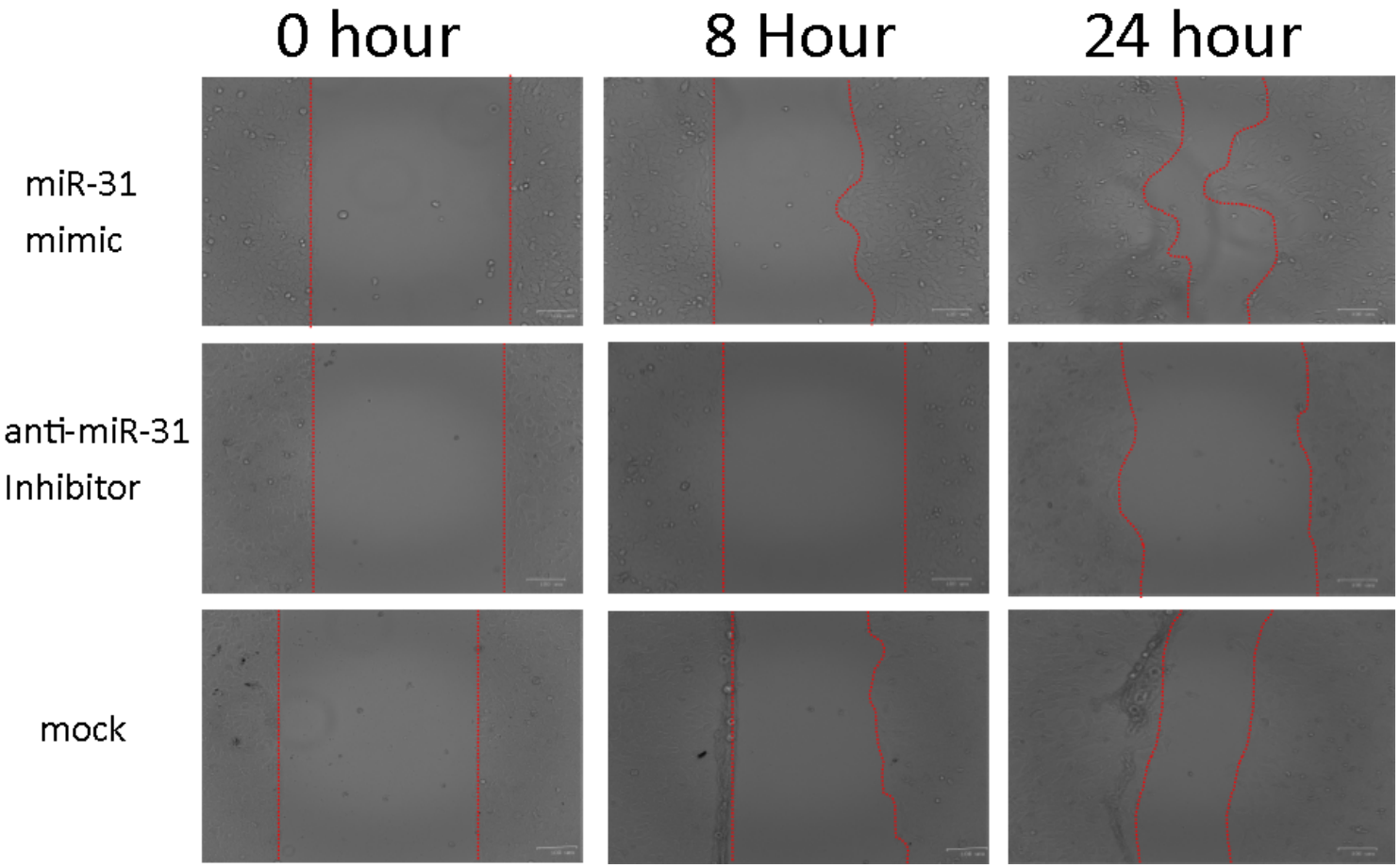

Figure 14: Migration assay after 24-hour transfection of HaCaT. miR-31 mimic transfected cells (top row) had the most migration after 24 hours, followed by mock (third row), and anti-miR-31 transfected cells (second row). Migration assays were performed in triplicate with duplicates of cell type in each assay. Red lines indicate border of gap between cells.

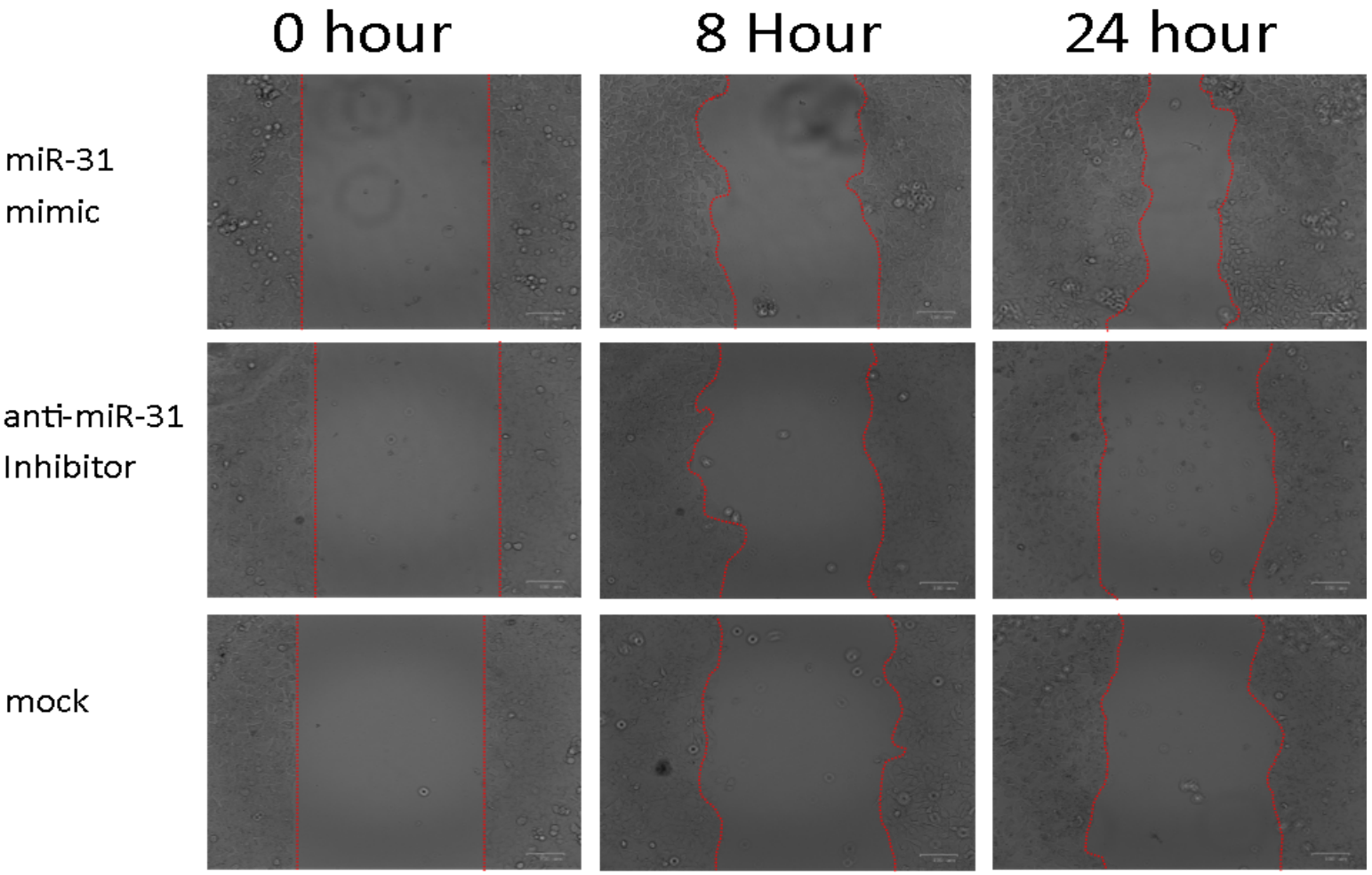

Figure 15: Migration assay after 24-Hour transfection of SRB-12. SRB-12 miR-31 mimic transfected cells showed the most amount of closure after 24 hours. Mock and anti-miR-31 transfected cells showed similar amounts of closure at the 8 and 24-hour time points. Migration assays were performed in triplicate with duplicates of transfection type in each assay. Red lines indicate border of gap between cells.

CHAPTER 6: DISCUSSION

Cutaneous squamous cell carcinoma is the second most common form of skin cancer in the Caucasian population [1]. Metastatic cSCC is rare, but with cSCC incidence on the rise and the high mortality of aggressive cSCC, studying the development of metastasis in cSCC is a worthy endeavor. Past studies with microRNAs in the Toland lab sparked further inquiry in this study into miR-31's role in metastatic cSCC.

The main hypothesis of this study was that miR-31 is important for cSCC metastasis. After a literature and database search of miR-31 targets, the hypothesis was refined to include that miR-31 regulates genes in the p38/MAPK pathway that are responsible for characteristics of metastasis and tumor characteristics like cell migration and invasion. There were two specific aims of this study:

1. To determine if there is a link between increased miR-31 expression and metastatic phenotypes.
2. To determine if there is a link between miR-31 and genes expressed in the p38/MAPK pathway.

6.1 miR-31 is upregulated in cSCC cell lines

After quantification of miR-31 by qPCR, I found that miR-31 has higher expression in cSCC cell lines, SRB-12 and COLO-16, as compared to HaCaT cells. HaCaT cells are human immortalized keratinocytes that model a normal, non-cancerous cell line. The greater expression of miR-31 in cell lines derived from tumors is consistent with my hypothesis that miR-31 may play a role in cancer phenotypes.

6.2 *LIMK2* expression is downregulated in HaCaT cells transfected with miR-31

Nine genes associated with the p38/MAPK pathway were investigated in this study. Genes were chosen because they were predicted to have miR-31 binding sites and an association with the p38/MAPK pathway. *MAPKAPK2, DUSP7, STAT3, MAP3K1, MAPK14, MAP2K4, MEF2A, LIMK2, and CREB1* expression were measured by qPCR in HaCaT cells. Results of these experiments showed no differences in expression of *MAPKAPK2, DUSP7, STAT3, MAP3K1, MAPK14, MAP2K4,* or *CREB1* between cells transfected with miR-31 or anti-miR 31. *MEF2A* and *LIMK2* showed 1.3-fold and 1.6-fold lower expression in miR-31 mimic transfected cells compared to the anti-miR-31 transfected cells, respectively (Figure 8). This suggests that miR-31 may target *MEF2A* and *LIMK2* mRNAs for degradation. [7,8] miR-31 has mismatches present in the binding site of the 3' UTR of *LIMK2*, which could lead to miRNA repressing translation of *LIMK2* followed by mRNA degradation [8]. Due to its binding sites in the 3' UTR and higher expression compared to *MEF2A, LIMK2* was further investigated with two subsequent transfections and qPCRs to validate the trend shown. Initially, *LIMK2* showed a trend of 1.7-fold lower expression in miR-31 transfected cells compared to anti-miR-31 transfected cells. On the third experimental replicate, the association between lower *LIMK2* expression and miR-31 expression was no longer observed (Figure 9). This change in results could be due to HaCaT cells with a higher passage number being used at this stage in the study.

LIMK2 functions as a regulator of actin remodeling, which can play a role in cell motility [22]. With a hallmark of metastasis being movement of cancerous cells to different

regions of the body, cell motility influenced by LIMK2 could play a role in metastasis. In colorectal cancer, aggressive tumors have decreased *LIMK2* expression and an upregulation of miR-31. [13,24,25] The HaCaT keratinocyte cell line used in this study initially exhibited a similar tendency when transfected with miR-31; thus giving more indication that miR-31, *LIMK2*, and aggressive cancer phenotypes might be connected in the development of metastatic cSCC.

6.3 miR-31 promotes migration phenotype

The primary aim of this study was to investigate the role of miR-31 in metastatic phenotypes. Cell proliferation and migration were the two phenotypes evaluated. There was no evidence that miR-31 affects cell proliferation as measured by MTT assay (Figure 12). Triplicate migration assays, each containing technical duplicates of each transfection type, showed that miR-31 influences cell migration. In both HaCaT and SRB-12, miR-31 transfected cells had the most gap closure after 24 hours. In HaCaT cells, the anti-miR-31 had the least amount of closure and mock cells had an intermediate amount of closure after 24 hours. In SRB-12, the mock and anti-miR-31 had very similar amounts of gap closure after 24 hours. In a 2014 study, Wang et al. found similar results in miR-31 transfected UT-SCC-7, a SCC cancerous cell line, and scratch wound assays. [15]

While the migration phenotype is promoted by miR-31, there may be different mechanisms behind this in each cell lines. SRB-12 cells did not have as pronounced differences in migration between transfection types. These cells also showed no conclusive link between miR-31 and *LIMK2.* On the other hand, HaCaT cells showed a greater migration and a noticeable difference in migration between the miR-31 mimic,

anti-miR-31, and mock transfection types. Decreased LIMK2 expression could be producing a more exaggerated migration- one comparable to decreased LIMK2 expression leading to more aggressive tumors and EMT-induced metastasis in colorectal cancer. [24,25]

6.4 Study Strengths and Limitations

The scientific rigor was the main strength of this study. The transfections, qPCR quantification, and migration assays were all performed in triplicate. Each experiment contained biological replicates as well. The use of multiple cell lines was another strength to this study.

This study had a few limitations. Although multiple metastatic phenotypes were investigated, the invasion assay failed to work. Invasion assays were attempted with wild type HaCaT, SRB-12, and COLO-16 cell lines, but these cells failed to cross the Matrigel matrix in the assay and therefore further analysis with transfected cells was not performed. Although multiple candidate miR-31 target genes were evaluated by qPCR, most of these genes were not evaluated at the protein level. Thus, it is possible that they are miR-31 targets, but miR-31 binding influences translation and not stability of the mRNA. Another limitation was that no experiments were done to test whether there is evidence of miR-31 binding to the predicted miR-31 binding sites in *LIMK2*. Despite the results indicating that miR-31 promotes migration, the mechanism behind this phenotypic change is unknown.

CHAPTER 7: CONCLUSION AND FUTURE DIRECTIONS

In conclusion, miR-31 promotes the metastatic phenotype of cell migration, but not cell proliferation. This confirms previous results showing an effect of miR-31 on migration in SCC cell lines [15]. miR-31 upregulation in cSCC cell lines compared to a normal cell line provides circumstantial evidence that miR-31 may promote cancer phenotypes, and therefore, more phenotypic assays should be investigated. Of the nine original genes of interest, only *LIMK2* showed some limited evidence of being downregulated by miR-31 and only in HaCaT cells. However, as these results were not significant, it cannot be said that this is a definitive association. More transfections and quantification of gene expression are required.

Along with more phenotypic assays investigating the role of miR-31 in metastasis and *LIMK2* expression quantification, future directions should include replicating performed experiments in the third, more aggressive COLO-16 cell line. This will provide more evidence into miR-31's role in a cSCC cell line that has high miR-31 expression levels. miR-31-mediated regulation of *LIMK2* should also be investigated with a luciferase reporter gene assay. Also, experiments manipulating *LIMK2* expression and observing change in phenotypes will give greater insight into *LIMK2's* part in metastasis and cancer progression.

ACKNOWLEDGEMENTS

I would like to first thank my research advisor, Dr. Amanda Toland, for her support and guidance. Under her supervision, I have applied knowledge learned in my classes and without this, my biology degree would feel incomplete. Her patience in teaching me basic lab procedures and directing me through this project was very much appreciated. I admire her ability to be calm and collected in stressful situations. I plan to model her intelligence and expertise in her field as I move on in my career path.

Next, I would like to thank past and present members of the Toland Lab. Special thanks go out to Reena, Cara, and Johnny. They were instrumental in guiding me through new lab procedures and were always constant pillars of support. I also appreciate the comic relief offered when comparing “tragedies” in and out of the lab. I wish everyone success and hope to keep in touch after graduation.

I would also like to thank the Undergraduate Research Office at The Ohio State University. The presentation opportunities and funding they provided me as a part of their apprentice program was pivotal to creating my own research project.

Finally, I would like to thank my friends and family for supporting me throughout my undergraduate career. They were the ones that kept me sane through the ups and downs of post-graduate applications, research, and life in general.

Works Cited

1. Garcia-Zuazaga, J., & Olbricht, S. M. (2008). Cutaneous squamous cell carcinoma. *Advances in dermatology*, *24*, 33-57.
2. Muzic, J. G., Schmitt, A. R., Wright, A. C., Alniemi, D. T., Zubair, A. S., Olazagasti Lourido, J. M., Sosa Seda, I. M., Weaver, A. L., & Baum, C. L. (2017). Incidence and Trends of Basal Cell Carcinoma and Cutaneous Squamous Cell Carcinoma: A Population-Based Study in Olmsted County, Minnesota, 2000 to 2010. *Mayo Clinic proceedings*, *92*(6), 890–898.
   Leibovitch, I., Huilgol, S. C., Selva, D., Hill, D., Richards, S., & Paver, R. (2005). Cutaneous squamous cell carcinoma treated with Mohs micrographic surgery in Australia I. Experience over 10 years. *Journal of the American Academy of Dermatology*, *53*(2), 253-260.
3. Hameetman, L., Commandeur, S., Bavinck, J. N., Wisgerhof, H. C., de Gruijl, F. R., Willemze, R., Mullenders, L., Tensen, C. P., & Vrieling, H. (2013). Molecular profiling of cutaneous squamous cell carcinomas and actinic keratoses from organ transplant recipients. *BMC cancer*, *13*, 58.
4. Cassarino, D. S., DeRienzo, D. P., & Barr, R. J. (2006). Cutaneous squamous cell carcinoma: a comprehensive clinicopathologic classification: part two. *Journal of cutaneous pathology*, *33*(4), 261-279.
5. Ratushny, V., Gober, M. D., Hick, R., Ridky, T. W., & Seykora, J. T. (2012). From keratinocyte to cancer: the pathogenesis and modeling of cutaneous squamous cell carcinoma. *The Journal of clinical investigation*, *122*(2), 464–472.
6. Karia, P., Han, J., Schmults, C. (2013). Cutaneous squamous cell carcinoma: estimated incidence of disease, nodal metastasis, and deaths from disease in the United States, 2012. *J AM Acad Dermatol.* 68, 957.
7. O'Brien, J., Hayder, H., Zayed, Y., & Peng, C. (2018). Overview of MicroRNA Biogenesis, Mechanisms of Actions, and Circulation. *Frontiers in endocrinology*, *9*, 402.
8. Hammond S. M. (2015). An overview of microRNAs. *Advanced drug delivery reviews*, *87*, 3–14.
9. Hoffmann, T. W., Duverlie, G., & Bengrine, A. (2012). MicroRNAs and hepatitis C virus: toward the end of miR-122 supremacy. *Virology journal*, *9*, 109.
10. Calin, G. A., & Croce, C. M. (2006). MicroRNA signatures in human cancers. *Nature reviews cancer*, *6*(11), 857-866.
11. Luo, L. J., Yang, F., Ding, J. J., Yan, D. L., Wang, D. D., Yang, S. J., ... & Wu, J. Z. (2016). MiR-31 inhibits migration and invasion by targeting SATB2 in triple negative breast cancer. *Gene*, *594*(1), 47-58.
12. Liu, C. J., Tsai, M. M., Hung, P. S., Kao, S. Y., Liu, T. Y., Wu, K. J., ... & Chang, K. W. (2010). miR-31 ablates expression of the HIF regulatory factor FIH to activate the HIF pathway in head and neck carcinoma. *Cancer research*, *70*(4), 1635-1644.
13. Zhang, W. W., Ming, X. L., Rong, Y., Huang, C. Q., Weng, H., Chen, H., ... & Wang, F. B. (2019). Diagnostic Value Investigation and Bioinformatics Analysis of miR-31 in Patients with Lymph Node Metastasis of Colorectal Cancer. *Analytical Cellular Pathology*, *2019*.
14. García-Sancha, N., Corchado-Cobos, R., Pérez-Losada, J., & Cañueto, J. (2019). MicroRNA Dysregulation in Cutaneous Squamous Cell Carcinoma. *International journal of molecular sciences*, *20*(9), 2181.
15. Wang, A., Landén, N. X., Meisgen, F., Lohcharoenkal, W., Ståhle, M., Sonkoly, E., & Pivarcsi, A. (2014). MicroRNA-31 is overexpressed in cutaneous squamous cell carcinoma and regulates cell motility and colony formation ability of tumor cells. *PloS one*, *9*(7), e103206.
16. Zhang, W., & Liu, H. T. (2002). MAPK signal pathways in the regulation of cell proliferation in mammalian cells. *Cell research*, *12*(1), 9-18.
17. Morrison D. K. (2012). MAP kinase pathways. *Cold Spring Harbor perspectives in biology*, *4*(11), a011254.
18. Brutkiewicz R. R. (2016). Cell Signaling Pathways That Regulate Antigen Presentation. *Journal of immunology (Baltimore, Md. : 1950)*, *197*(8), 2971–2979.
19. del Barco Barrantes, I., & Nebreda, A. R. (2012). Roles of p38 MAPKs in invasion and metastasis.

20. Kalluri, R., & Weinberg, R. A. (2009). The basics of epithelial-mesenchymal transition. *The Journal of clinical investigation*, *119*(6), 1420–1428.
21. Kobayashi, M., Nishita, M., Mishima, T., Ohashi, K., & Mizuno, K. (2006). MAPKAPK-2-mediated LIM-kinase activation is critical for VEGF-induced actin remodeling and cell migration. *The EMBO journal*, *25*(4), 713–726. https://doi.org/10.1038/sj.emboj.7600973
22. Acevedo, K., Moussi, N., Li, R., Soo, P., & Bernard, O. (2006). LIM kinase 2 is widely expressed in all tissues. *Journal of Histochemistry & Cytochemistry*, *54*(5), 487-501.
23. Su, J., Zhou, Y., Pan, Z., Shi, L., Yang, J., Liao, A., ... & Su, Q. (2017). Downregulation of LIMK1–ADF/cofilin by DADS inhibits the migration and invasion of colon cancer. *Scientific reports*, *7*, 45624.
24. Kobayashi, M., Nishita, M., Mishima, T., Ohashi, K., & Mizuno, K. (2006). MAPKAPK-2-mediated LIM-kinase activation is critical for VEGF-induced actin remodeling and cell migration. *The EMBO journal*, *25*(4), 713-726.
25. Zhang, Y., Li, A., Shi, J., Fang, Y., Gu, C., Cai, J., ... & Liu, S. (2018). Imbalanced LIMK1 and LIMK2 expression leads to human colorectal cancer progression and metastasis via promoting β-catenin nuclear translocation. *Cell death & disease*, *9*(7), 1-10.
26. Vlecken, D. H., & Bagowski, C. P. (2009). LIMK1 and LIMK2 are important for metastatic behavior and tumor cell-induced angiogenesis of pancreatic cancer cells. *Zebrafish*, *6*(4), 433-439.
27. Sumi, T., Matsumoto, K., & Nakamura, T. (2001). Specific activation of LIM kinase 2 via phosphorylation of threonine 505 by ROCK, a Rho-dependent protein kinase. *Journal of Biological Chemistry*, *276*(1), 670-676.
28. Radu, M., Semenova, G., Kosoff, R., & Chernoff, J. (2014). PAK signalling during the development and progression of cancer. *Nature reviews. Cancer*, *14*(1), 13–25.
29. Molli, P. R., Li, D. Q., Murray, B. W., Rayala, S. K., & Kumar, R. (2009). PAK signaling in oncogenesis. *Oncogene*, *28*(28), 2545–2555. https://doi.org/10.1038/onc.2009.119
30. Parikh, S. A., Patel, V. A., & Ratner, D. (2014). Advances in the management of cutaneous squamous cell carcinoma. *F1000prime reports*, *6*, 70.
31. Jennings, L., & Schmults, C. D. (2010). Management of high-risk cutaneous squamous cell carcinoma. *The Journal of clinical and aesthetic dermatology*, *3*(4), 39–48.
32. Rowe, D. E., Carroll, R. J., & Day Jr, C. L. (1992). Prognostic factors for local recurrence, metastasis, and survival rates in squamous cell carcinoma of the skin, ear, and lip: implications for treatment modality selection. *Journal of the American Academy of Dermatology*, *26*(6), 976-990.
33. Breuninger, H., Schaumburg-Lever, G., Holzschuh, J., & Horny, H. P. (1997). Desmoplastic squamous cell carcinoma of skin and vermilion surface: a highly malignant subtype of skin cancer. *Cancer*, *79*(5), 915-919.
34. Stratigos, A., Garbe, C., Lebbe, C., Malvehy, J., Del Marmol, V., Pehamberger, H., ... & Middleton, M. R. (2015). Diagnosis and treatment of invasive squamous cell carcinoma of the skin: European consensus-based interdisciplinary guideline. *European journal of cancer*, *51*(14), 1989-2007.
35. Miller, D. L., & Weinstock, M. A. (1994). Nonmelanoma skin cancer in the United States: incidence. *Journal of the American Academy of Dermatology*, *30*(5), 774-778.
36. Rock, A.N., Fisher, M.D., Amborski, G., Allain, D.C., Klee, V., Peters, S.B., Kang, S., Toland, A.E. (2020). MicroRNA expression profiling of cutaneous squamous cell carcinomas arising in different sites. *Otolaryngology-Head and Neck Surgery.* Manuscript submitted for publication.
37. You, T., Gao, W., Wei, J., Jin, X., Zhao, Z., Wang, C., & Li, Y. (2015). Overexpression of LIMK1 promotes tumor growth and metastasis in gastric cancer. *Biomedicine & Pharmacotherapy*, *69*, 96-101.
38. Liu, B., Yang, L., Huang, B., Cheng, M., Wang, H., Li, Y., ... & Ji, W. (2012). A functional copy-number variation in MAPKAPK2 predicts risk and prognosis of lung cancer. *The American Journal of Human Genetics*, *91*(2), 384-390.

39. Teng, C. H., Huang, W. N., & Meng, T. C. (2007). Several dual specificity phosphatases coordinate to control the magnitude and duration of JNK activation in signaling response to oxidative stress. *Journal of Biological Chemistry*, *282*(39), 28395-28407.
40. Xiong, H., Du, W., Sun, T. T., Lin, Y. W., Wang, J. L., Hong, J., & Fang, J. Y. (2014). A positive feedback loop between STAT3 and cyclooxygenase-2 gene may contribute to Helicobacter pylori-associated human gastric tumorigenesis. *International journal of cancer*, *134*(9), 2030-2040.
41. Pearlman, A., Loke, J., Le Caignec, C., White, S., Chin, L., Friedman, A., Warr, N., Willan, J., Brauer, D., Farmer, C., Brooks, E., Oddoux, C., Riley, B., Shajahan, S., Camerino, G., Homfray, T., Crosby, A. H., Couper, J., David, A., Greenfield, A., … Ostrer, H. (2010). Mutations in MAP3K1 cause 46,XY disorders of sex development and implicate a common signal transduction pathway in human testis determination. *American journal of human genetics*, *87*(6), 898–904.
42. Xiao, Y., Wang, J., Yan, W., Zhou, K., Cao, Y., & Cai, W. (2017). p38α MAPK antagonizing JNK to control the hepatic fat accumulation in pediatric patients onset intestinal failure. *Cell death & disease*, *8*(10), e3110.
43. Ding, L., Yu, L. L., Han, N., & Zhang, B. T. (2017). miR-141 promotes colon cancer cell proliferation by inhibiting MAP2K4. *Oncology letters*, *13*(3), 1665-1671.
44. Lyons, M. R., Schwarz, C. M., & West, A. E. (2012). Members of the myocyte enhancer factor 2 transcription factor family differentially regulate Bdnf transcription in response to neuronal depolarization. *The Journal of neuroscience : the official journal of the Society for Neuroscience*, *32*(37), 12780–12785.
45. Oerlecke, I., Bauer, E., Dittmer, A., Leyh, B., & Dittmer, J. (2013). Cyclic AMP enhances TGFβ responses of breast cancer cells by upregulating TGFβ receptor I expression. *PloS one*, *8*(1).
46. Côté, M. C., Lavoie, J. R., Houle, F., Poirier, A., Rousseau, S., & Huot, J. (2010). Regulation of vascular endothelial growth factor-induced endothelial cell migration by LIM kinase 1-mediated phosphorylation of annexin 1. *The Journal of biological chemistry*, *285*(11), 8013–8021.
47. Vidyasagar, A., Wilson, N. A., & Djamali, A. (2012). Heat shock protein 27 (HSP27): biomarker of disease and therapeutic target. *Fibrogenesis & tissue repair*, *5*(1), 7.
48. Keyse, S. M. (2008). Dual-specificity MAP kinase phosphatases (MKPs) and cancer. *Cancer and Metastasis Reviews*, *27*(2), 253-261.
49. Riebe, C., Pries, R., Schroeder, K. N., & Wollenberg, B. (2011). Phosphorylation of STAT3 in head and neck cancer requires p38 MAPKinase, whereas phosphorylation of STAT1 occurs via a different signaling pathway. *Anticancer research*, *31*(11), 3819-3825.
50. Pham, T. T., Angus, S. P., & Johnson, G. L. (2013). MAP3K1: Genomic Alterations in Cancer and Function in Promoting Cell Survival or Apoptosis. *Genes & cancer*, *4*(11-12), 419–426.
51. Osaki, L. H., & Gama, P. (2013). MAPKs and signal transduction in the control of gastrointestinal epithelial cell proliferation and differentiation. *International journal of molecular sciences*, *14*(5), 10143–10161.
52. Ahn, Y. H., Yang, Y., Gibbons, D. L., Creighton, C. J., Yang, F., Wistuba, I. I., Lin, W., Thilaganathan, N., Alvarez, C. A., Roybal, J., Goldsmith, E. J., Tournier, C., & Kurie, J. M. (2011). Map2k4 functions as a tumor suppressor in lung adenocarcinoma and inhibits tumor cell invasion by decreasing peroxisome proliferator-activated receptor γ2 expression. *Molecular and cellular biology*, *31*(21), 4270–4285.
53. Potthoff, M. J., & Olson, E. N. (2007). MEF2: a central regulator of diverse developmental programs. *Development*, *134*(23), 4131-4140.
54. Delghandi, M. P., Johannessen, M., & Moens, U. (2005). The cAMP signalling pathway activates CREB through PKA, p38 and MSK1 in NIH 3T3 cells. *Cellular signalling*, *17*(11), 1343-1351.